Fiber Reinforced Plastic
Pressure Vessels

Wafaa Ishak

A Major Technical Report

in

The Department

of

Mechanical Engineering

Presented in Partial Fulfillment of the Requirements
for the Degree of Master of Engineering at
Concordia University
Montréal, Québec, Canada

May 1985

ABSTRACT

Fiber Reinforced Plastic
Pressure Vessels

Wafaa Ishak

A survey of recent advances on fiber reinforced plastic pressure vessels is presented. It covers the matrices and reinforcing fibers, vessel compositions, fabrications and structural analysis. Some specification and qualification requirements from different user and certifying agencies are also included.

ACKNOWLEDGEMENTS

Special thanks are due to my supervisor at Concordia University, Dr. S.V. Hoa for his guidance and encouragement received over the duration of the study.

I also wish to acknowledge the patience and understanding exhibited by my wife during preparation of this report.

CONTENTS

LIST OF FIGURES

LIST OF TABLES

NOMENCLATURE

E	Modulus of Elasticity
G	Modulus of Rigidity
M	Bending Moment
N	Membrane Force per Unit Length
Q	Transverse Shear Force per Unit Length
α	Fibre angle relative to a meridian
γ	Shear Strain
ϵ	Direct Strain
μ	Poisson's Ratio
σ	Direct Stress
τ	Shear Stress
θ	Fibre Angle relative to the 'hoop' direction.

All other variables are defined as they appear in the text.

MATRIX NOTATION

$\| \ \|$	Column Matrix
$[\ ]$	Square Matrix

CHAPTER (1)

INTRODUCTION

1. INTRODUCTION

The utilization of composite materials has progressed significantly over the past two decades, this is due to the fact that composite materials have high stiffness and strength, low density, damage tolerance and good fatigue response characteristics, good corrosion resistance in hostile environments, and ease of fabrication. A comparison between the specific strength (strength density) of various composites and metals are shown in Table 1 and Figure 1.

The unique properties of composite materials have led to their use in pressure vessels; replacing conventional metallic construction in many applications.

In the aerospace industry, composite material pressure vessels have been used in making oxygen tanks to meet weight objectives for long range aircraft [1].

A light weight fireman's breathing system cylinders have been evaluated by the fire department of New York, Los Angeles and Houston with excellent results [2].

Mountain climbers have found that using light weight composite cylinders is a major step forward in their carreer. Fiber reinforced plastic chemical resistance tanks have started taking their place in various chemical industries where highly corrosive fluids and gases need to be stored [3].

This report describes the materials which are used in making these vessels, the fabrication techniques and also the structural analysis for the calculation of stress and strain for design.

CHAPTER (2)

MATERIALS

2. MATERIALS

The characteristics of a fibrous composite are influenced by the properties of the fibers and the matrix (or binder) as well as by the nature of the interfacial bond between them. In the following paragraphs the most common polymeric matrix materials, fibers, and composite systems are described.

2.1 Polymeric Materices

The matrix has several functions: -

1. Acts as a bridge to hold the fibers in place.
2. Protects the filaments from damage by abrasion and chemical attack.
3. Transmits stresses.

There are two basic types of polymers, the thermoplastics and the thermosets. For fiber reinforced plastic vessels thermosets are usually used [4].

Thermosets develop a well bonded three dimensional molecular structure upon curing. The conditions necessary to effect cure and the characteristics of the uncured resin can be varied by changing the basic formulation.

Moreover, some thermosets can be held in a partially cured condition for prolonged periods of time. This inherent flexibility makes the thermosets ideally suited to use as matrix materials for the continuous fiber composites used in vessels. Of the thermosets, polyesters, epoxies and polyimides are perhaps the most widely used in FRP (fiber reinforced plastic) composites [6].

Polyester Resins

Polyester resins have the ability to cure or harden at room temperature under no pressure or low pressure when catalyzed. This characteristic allows the polyester resin to be used inexpensively in making vessels for the chemical processing industry. However these resins have the problem of large shrinkage during the curing process and relatively poorer chemical resistance as compared to the epoxy resins. Polyester resins are therefore restricted to commercial vessels and they gave way to epoxy resins in more critical applications [4].

Epoxies

Usually each epoxy contains the base resin, a curing agent, and in certain cases, a filler or thixotropic addition. Diluents, additives used to reduce the viscosity of the resin in the uncured state, are undesirable since they reduce both fatigue life and heat resistance of the cured resin. Processibility and properties of cured epoxy material are highly dependent on the type of hardener used to cure it. The curing reaction as the resin passes from the (A stage) through a partially cured state in which the epoxy exists as a thermoplastic (B stage) to final cure which is irreversible.

However, by controlling the temperature, one may maintain the resin in the B stage for prolonged periods of time. This flexibility makes possible the use of "prepregs" (pre-impregnated) fibers or fabrics in composite fabrication. The epoxies have superior chemical resistance, good adhesion to most substrates, very low water absorption and cure shrinkage, good electrical properties, and high strength as compared to polyester resins. Epoxy resins are among the most important of the matrix materials used in fiber reinforced vessels containing high pressure [4].

Polyimides

The polyimides are a special group of aromatic polymers designed to function at temperatures in excess of 260°C. Reaction of the starting constituents at low temperature produces high molecular weight polyamic acids which require a period of 30 minutes to as much as 4 hours for the formation to be completed. If application is not anticipated within a few hours the material must be kept in solution, sealed and refrigerated to prevent degradation. In final product form, the polyamic acid must be cured by heat treatment for a period of 5 to 16 hours at elevated temperatures to produce the polyimide. A new type of polyimide which circumvents some of the shortcomings of the condensation curing systems has recently been developed and is commercially available as an advanced formulation under the name of P13N. The P13N differs from conventional polyimide resin systems in that, during final molding at 320°C the reaction simultaneously fuses the plies together to form a coherent, compact, void-free (void content of less than 2 vol%) product [4].

2.2 Reinforcing Fibers

The fiber is the backbone of an advanced reinforced plastic composite. It carries the load and imparts stiffness to the structure. S-Glass, Carbon and Kevlar 49 fibers are the most widely used reinforcing fiber material in the application of composite pressure vessels.

The strength, modulus and density of the more common fibers used in reinforced plastics are shown in Table 2. Among these S-Glass, Carbon fiber and Kevlar 49 fiber are usually used in high pressure vessels.

S-Glass

S-Glass was developed as a commercially fiberizable glass with high strength and elastic modulus and good retention of strength at high temperatures. The density of S-Glass fibers is 2.5 g/cm^3 Young's modulus of as drawn S-Glass fibers at room temperature is

86×10^6 N/cm^2 and thermally compact S-Glass fibers have an elastic modulus of 9.3×10^6 N/cm^2 at room temperature. The average tensile strength of virgin S-Glass fibers is 450×10^3 N/cm^2 stressed to their ultimate strength, S-Glass fibers have an average elongation of 5.3 percent. The strength of S-Glass fibers is retained well with temperature although at 540°C plastic yielding of the fiber begins. The strain, annealing and softening points of S-Glass are 760, 810 and 970°C, its coefficient of thermal expansion near room temperature is 2.9 $\times 10^{-6}$ C^{-1}. Significant damage can occur to S-Glass roving stored at temperatures above 0°C unless the material is maintained under very low humidity conditions, in which case temperatures up to 25°C appear satisfactory [4].

Carbon Fiber

Most carbon fibers are provided by thermal decomposition of an organic precursor, usually rayon or polyacrylonitrile (PAN) although some are made from extruded pitch. Since the precursors are in multifiber strands, so are the carbon fibers produced from them. Commercially available forms are staples (relatively short length), as well as fibers and specialty materials like kints and felts. The final mechanical properties of carbon fibers are controlled by the processing parameters. The fiber modulus increases with heat treatment temperature from 1200 to 2500°C, whereas strength reaches a maximum over temperature range of 1400 to 1700°C, thus it is impossible to obtain ultra high strength and modulus in the same fiber. In addition to bare fibers, producers sell carbon fibers that are treated to provide more effective bonding with matrix materials, and thereby yield improved interlaminar shear strengths in composites. Typical properties of carbon fiber are shown in Table 3 [4].

PRD - 49 Fiber (Kevlar)

PRD-49 is a high strength, intermediate modulus organic fiber with excellent potential for reinforcement of polymeric materials. As is noted in table 4 two versions of PRD-49 are now available. The type III form is normally preferred as a reinforcement while type IV form is an important potential tire cord material expected to be competitive with steel wire. These fibers have very good handleability, for example, strength retention after weaving is 90 percent of the virgin yarn strength. The fibers are nonmelting and are about equal to Nomex nylon in flammability resistance (limiting oxygen index of 0.29). The fibers possess moderate temperature resistance. The tensile strength drops about 30 percent after 450 hours exposure to 240°C in air. PRD-49 is also quite resistant to most acids, bases and solvents.

The fibers do, under certain conditions, pick up moisture, with an accompanying length change [4].

2.3 Fiber/Matrix Properties Combined

The properties of a fibrous composite depend not only on the identities and relative quantities of the fiber and resin used, but also on the way how the combination is made, table 5 shows the differences obtained by different combinations of short or long fibers with resins. In addition, a unidirectional composite, one in which all fibers are aligned in parallel, has the highest strength and stiffness in the fiber direction for a given fiber/matrix system. Typical unidirectional properties for the more important composites are compared in Table 6. However, as shown in Figure 2, such a composite will have rather poor properties if stressed at some angle oblique to the fiber direction. A 0/90 or crossplied laminate has half of the fibers aligned in one direction and half at 90 degrees. The stress angle versus strength profile for such a laminate is also shown in Figure 2. By adding still more fiber directions, ~~e.g.~~ in a 0/±45/90 or 0/±60 degrees laminate, a pseudoisotropic profile can be achieved.

The properties of E and S-glass composites are compared in Table 7. The S-glass produces composites that are superior in all respects.

Because carbon fibers are available in such wide variety, there is a broad spectrum of attainable composite properties. Table 8 lists some typical composite properties for the various types of carbon fibers in epoxy [5]. Data for two polyimide matrix systems are included for comparison. The carbon/polyimide composites are lower in strength than comparable carbon/epoxies. Some properties of Kevlar PRD-49/epoxy composites are summarized in Table 9. The low compressive strength indicates that the greatest potential for PRD-49 lies in its use in structures loaded in pure tension such as pressure vessels [5].

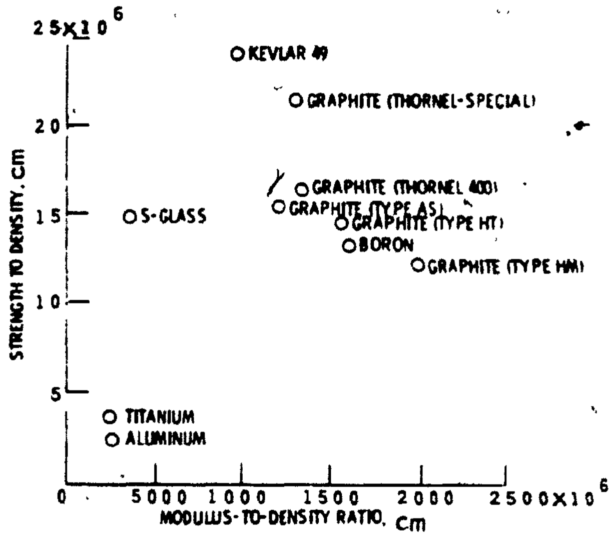

Figure 1 - Strength-to-density and modulus-to-density ratios of fiber/epoxy strand properties (based on tensile strength tests of epoxy resin-impregnated strain specimens). [4]

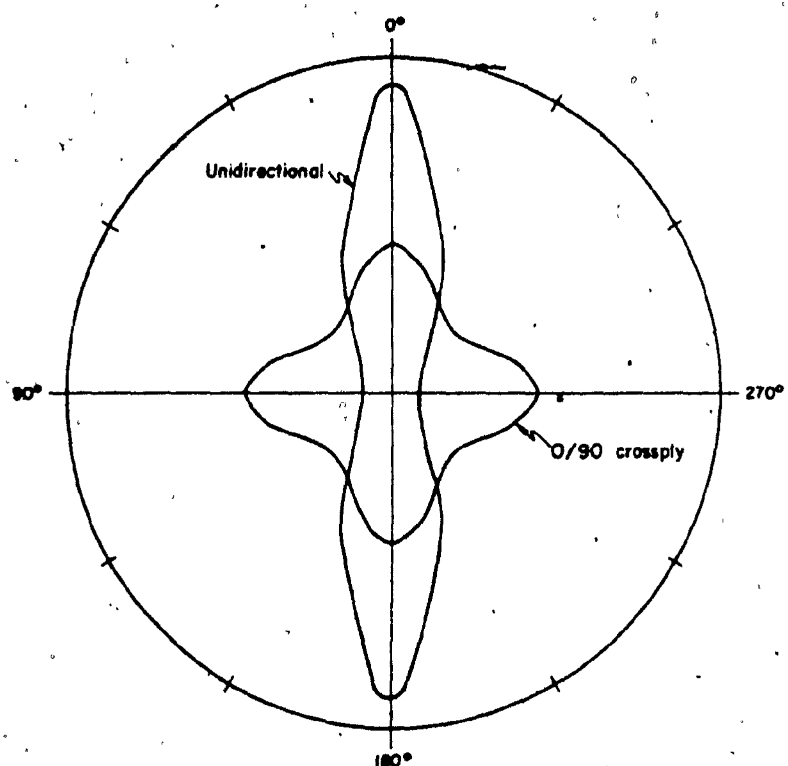

FIGURE 2 STRENGTH vs. STRESS ANGLE FOR GLASS-FIBER REINFORCED PLASTIC COMPOSITE [4]

Fiber content — nominal 65 volume percent.

TABLE 1 MATERIAL SPECIFIC STRENGTHS.

[7]

MATERIAL	SPECIFIC STRENGTH $\hat{\sigma}_m$ × 10^6
R.A.E. C.F.R.P. TYPE 1	7.04
R.A.E. C.F.R.P. TYPE 2	8.94
THORNEL C.F.R.P. 75S	10.07
HERCULES C.F.R.P. HTS	9.60
DU PONT PRD. 49 (KEVLAR)	8.69
BORON R.P.	6.78
SCOTCHPLY G.F.R.P. TYPE 1002	8.15
R.A.E. G.F.R.P.	6.76
3.M. G.F.R.P. 3M - XP215S	6.75
AL ALLOY 2L.63	1.65
AL ALLOY DTD 5074	1.99
MG ALLOY DTD 5031	1.67
MAR AGEING STEEL	2.72

TABLE 2 PROPERTIES OF THE MORE COMMON FIBERS USED IN REINFORCED PLASTICS [4]

Material	Tensile Strength, ($N/cm^2 \times 10^3$)	Modulus, ($N/cm^2 \times 10^6$)	Density (g/cm^3)
E Glass	345	7.2	2.55
S Glass	450	8.6	2.50
PRD-49-III	275	13	1.45
Boron	275-310	38-41	2.4
Carbon	103-310	69-62	1.4-1.9
Steel Wire	206-512	20	7.7-7.8

TABLE 3 TYPICAL PROPERTIES OF CARBON FIBERS [6]

Vendor (Trade Name)	Grade	Precursor(a)	Tensile Strength, N/cm² x 10³	Tensile Modulus, N/cm² x 10⁶	Density, g/cm³	Form
Union Carbide (Thornel)	T-25	R	125	17	1.43	2 ply yarn
	T-40	R	172	28	1.56	2 ply yarn
	T-50	R	207	35	1.65	2 ply yarn
	T-75	R	252	52	1.82	2 ply yarn
	T-400	P	310	21	1.78	1 ply yarn
Hitco	HMG-25	R	103	17	1.5	yarn
	HMG-40	R	172	28	1.7	yarn
	HMG-50	R	207	35	1.8	yarn
Celanese (Celion)	GY-70	P	207	52	1.9	--
Hercules/Courtaulds (Grafil) (Magnamite)	A	P	269	21	1.8	10,000 tow
	HM(b)	P	207	38	1.86	10,000 tow
	HT(b)	P	241	28	1.72	10,000 tow
Great Lakes (Fortafil)	3-T	P	172	19	1.76	150,000 tow
	4-T	P	241	25	1.78	50,000 tow
	5-T	P	276	33	1.79	--
	6-T	P	290	41	1.9	50,000 tow
Whittaker/Morganite (Modmor)	I	P	172	41	2.0	10,000 tow
	II	P	276	28	1.76	10,000 tow
Polycarbon	A	P	207	24	1.75	tow
	T	P	241	28	1.75	tow
	M	P	207	41	1.90	tow
Kureha	Corbis	T	51-172	2.7-26	1.6-1.7	--
Tokai (Thermalon)	T-S	P	159	48	2.0	--
Stackpole (Panex)	30	P	275-324	21	--	160,000 tow
Nippon	G.L	L	58	--	1.8	--
Sigri (Sigrafil)		P	148-245	19-48	1.8-2.0	--

(a) R = Rayon P = Polyacrylonitrile L = Lignin
Source: Manufacturers' Literature

(b) Surface-treated versions also available under designations HM-S and HT-S

TABLE 4 PROPERTIES OF PRD-49 FIBERS [6]

	Type III	Type IV
Diameter	0.11 mm	0.11 mm
Density	1.45 g/cm^3	1.45 g/cm^3
Tensile Strength	276 x 10^3 N/cm^2	296 x 10^3 N/cm^2
Tensile Modulus	13 x 10^6 N/cm^2	8.3 x 10^6 N/cm^2
Stress-Strain Curves	Linear	Non-Linear
Elongation	2.0%	3.3%
Moisture Regain	1.5%	4.0%

TABLE 5 TYPICAL COMPOSITE EFFICIENCIES ATTAINED IN REINFORCED PLASTICS [4]

Fiber Configuration		Fiber Length	Total Fiber Content (by volume) V_f	F_{long} (a) N/cm² x 10³ F_{theor} (b)	F_{test} (c)	Composite Efficiency (d) %
Filament-wound (unidirectional)	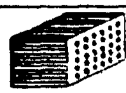	Continuous	0 77	214	124	58.0
Cross Laminated Fibers	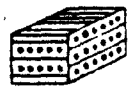	Continuous	0 48	136	50.0	36.8
Cloth Laminated Fibers	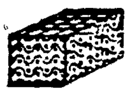	Continuous	0 46	136	29.6	21 8
Mat Laminated Fibers		Continuous	0 48	136	39.4	29.0
Chopped Fiber Systems (random)		Non-continuous	0 13	41 8	10.3	24 7
Glass Flake Composites		Non-continuous	0 70	114.1	13.8	12.1

(a) F_{long} = Ultimate tensile strength in direction of greatest fiber content (longitudinal), if there is one

(b) Theoretical strength based on "Rule of Mixtures"

$$F_{theor} = V_f S_f + (1 - V_f) S_m$$

where

S_f = 400 (275.8) ksi (N/cm² x 10³) – typical boron or carbon fiber strength

S_m = 10 (6 9) ksi (N/cm² x 10³) – typical resin strength

(c) F_{test} = typical experimental strength values

(d) Composite efficiency = $(F_{test}/F_{theor}) \times 100$

TABLE 6 TYPICAL LONGITUDINAL(a) PROPERTIES OF UNIDIRECTIONAL REINFORCED-PLASTIC COMPOSITES [6]

Fiber	Matrix	Ultimate Tensile Strength $N/cm^2 \times 10^3$	Tensile Modulus $N/cm^2 \times 10^6$	Ultimate Compressive Strength $N/cm^2 \times 10^3$
E glass	Epoxy	103-172	4-5 5	60
S glass	Epoxy	172-200	6.6	138
PRD-49	Epoxy	144	8 6	28-41
Boron	Epoxy	124-144	21-22	275-303
Boron	Polyimide	117-131	~21-21.4	--
Carbon(b)	Epoxy	41-138	12-21	41-138
Carbon(c)	Polyimide	124-144	16	120
Steel	Epoxy	206-293	10-15	--

(a) parallel to the fiber direction

(b) various fibers

(c) Modmor II only

TABLE 7 COMPARISON OF E- AND S-GLASS/EPOXY[a] ROOM TEMPERATURE PROPERTIES AT 0° STRESS ANGLE [4]

	Laminate Construction			
	Unidirectional (0°)		Cross Plied (0/90°)	
Property	E glass	S glass	E glass	S glass
Flexural Strength $N/cm^2 \times 10^3$	114	121	82 7	96.5
Flexural Modulus $N/cm^2 \times 10^6$	3.6	4.0	2.4	2.6
Tensile Strength $N/cm^2 \times 10^3$	110	134	52	68
Tensile Modulus $N/cm^2 \times 10^6$	3.9	4 4	2.6	2.7
Compression Strength $N/cm^2 \times 10^3$	62	69	52	57

(a) Fiber content — nominal 65 volume percent

TABLE 8 TYPICAL TENSILE PROPERTIES OF CARBON-FIBER COMPOSITES AT ROOM TEMPERATURES [4]

Fiber Description	Matrix	Laminate Orientation, degrees	Ultimate Tensile Strength, N/cm^2 x 10^3	Modulus, N/cm^2 x 10^6
HT	Epoxy	0	130	14
		90	1.7	0.80
		0/±45	79.0	9.00
HM	Epoxy	0	72.0	17
		90	4.7	0.80
		±45	15	1.7
		0/90	37	10.0
A	Epoxy	0	116	13.6
GY-70	Epoxy	0	62	29
		90	2	0.60
Fortafil 5Y	Polyimide	0	63	16.3(a)
		90	2.0	--
HMG-50	Polyimide	0	48.0	17.8
		90	1.8	--

(a) In flexure

TABLE 9
PROPERTIES OF PRD-49/EPOXY LAMINATES [4]

Density	1.38 g/cm^3
Interlaminar Shear Strength, dry	6200 N/cm^3
Interlaminar Shear Strength, after 3 day water boil	5510 N/cm^2
Tensile Strength	165 N/cm^2 x 10^3
Tensile Modulus	1.5 x 10^6 N/cm^2
Charpy Impact Strength (transverse to fibers)	860 joules/cm^2
Fatigue Strength, 10^7 cycles	14 N/cm^2 x 10^3
1000 hr Rupture Strength at Room Temperature	124 N/cm^2 x 10^3
Compressive Strength(a)	20-34 N/cm^2 x 10^3

(a) Data for composites containing Type I fiber, the laboratory version of the current Type III production fiber.

CHAPTER (3)

STRUCTURAL AND FABRICATION DETAILS

3.1 Vessel Composition

Filament wound composite vessels utilizing high strength-to-density and modulus-to-density ratio materials offer significant weight savings over conventional all-metal pressure vessels for containment of high pressure gases and fluids.

The structural efficiencies of the all metal pressure vessels range from 0.7 to 1.5 x 10^4 meters based on a pressure vessel performance factor (P_bV/W) where P_b is the burst pressure, V is the contained volume, and W is the vessel weight. In comparisons filament wound (FW) composite pressure vessels are capable of yielding performance factor values ranging from 2.0 to 3.0 x 10^4 meters when made using advanced fiber/resin composites and equipped with metallic liners. FW composite pressure vessels can therefore provide greater structural efficiencies (hence lower weight) than all metallic pressure vessels of similar volume and pressure rating. This desirable characteristic derives from the high strength of the continuous fibers, Figure 3 [6].

Composite pressure vessels for high performance applications are designed to load the fibers in the composite overwrap to high stress levels (ranging from 60 to 70 percent of fiber ultimate strength). However, high fiber stress levels result in significant elongations of the composite (0.5 to 2.0 percent) and extensive crazing or cracking of the resin matrix between the fibers.

Resin crazing generally becomes significant at a composite stress between about 10 to 40 percent of ultimate fiber strength which is considerably lower than the operating stress of high performance composite pressure vessels. The resin matrix craze paths can join to provide a leak path shown schematically in Figure 3. For this reason apart from the high strength filament winding layer, an internal liner must then be provided to prevent leakage of the contained fluid or gas. The basic composition of a high pressure vessel therefore consists of a high strength filament winding layer plus an impermeable liner. The filament winding layer consists of continuous fibers and resin as discussed earlier.

The liner must be both chemically compatible with and impermeable to the contained fluid or gas. The liner also must be capable of straining or elongating with the composite during pressurization and of returning to a stable and non-buckled position after pressure is reduced in the vessel. Three classes of liners used are:-

<u>Elastomeric</u> - For near ambient temperature applications where some permeability is permissible.

<u>Thin Metal</u> - Bonded to the overwrap - the lightest weight vessel, but cyclic life limited.

Load Sharing Metal - Thick metal liner is used, shares in supporting structural load.

3.1.1 Elastomeric Lined Composite Pressure Vessels

Conventional low pressure composite pressure vessels (3.5-17 N/cm^2) generally operate at fiber stress levels of 10 percent or less of fiber ultimate strengths. Such low pressure structures do not need to be equipped with special liners because of the resultant low elongation levels. A resin rich gel coat applied to the internal surface of the composite vessel serves as an impermeable liner to contain fluid or gas.

An example of the elastomeric liner vessel is the filament wound Kevlar 49/epoxy composite pressure vessel (shown in Figure 4) which has been developed by Lawrence Livermore Laboratory (LLL) under National Aeronautics and Space Administration (NASA) and Energy Research and Development Administration (ERDA) interagency agreement. Development test results for this vessel are shown in Table 10 [6].

3.1.2 Thin Metal Lined Composite Pressure Vessel

In applications where a light weight vessel design is desired and elastomeric liners are unacceptable (cryogenic temperature and/or high pressure gas service) a light weight liner must be used.

The thin liner concept utilizes the high strength composite overwrap as the primary load carrying element of the structure. A metal liner of the minimum thickness and weight is used as a leakage barrier. The liner contributes negligible weight and load carrying capability.

The choice of a suitable metallic liner material is difficult in cases where the vessel must be designed for high cyclic life. The thin metal liners are subjected to severe plastic straining during pressure cycling, as shown in Figure 5. The liner must be capable of withstanding both high plastic tensile and compressive strains while providing a reasonable cyclic life. Because the liner is forced into compression upon depressurization of the vessel, the liner must be well bonded to the inside wall of the composite overwrap in order to prevent the formation of wrinkles and disbonded areas which can result in leakage during subsequent pressure cycles.

The liner material must have the capability of being readily processed and welded into impermeable liner assemblies. An example of the aluminum liner vessel is shown in Figures 6, 7 and 8.

The thin metal lined composite pressure vessel concept has been extensively evaluated in various programs. The results and success of these programs have depended greatly upon the selection of suitable composite overwrap and liner materials.

Ideally, the composite overwrap should be made from light weight, high modulus fibers and the liners should be made from low to medium modulus, high yield strength (high elastic strain capability) metal foils. Table 11 shows comparison in the extensibility of various vessel overwrap and liner materials.

The strength-to-density versus the modulus-to-density ratios for a number of the advanced fibers are shown in Figure 1 [6].

The advanced fibers have significantly higher modulus-to-density ratios than do S-glass fibers and have generally provided the best approach for fabrication of light weight, high cyclic life, thin metal lined composite pressure vessels. Development test results for some thin metallic lined vessels are shown in Tables 12 and 13. A comparison between different metallic vessel and metallic lined vessel with filament would overwrap are shown in Figure 9 and 10.

3.1.3 Composite Pressure Vessels With Load Sharing Liners

The load sharing liner concept utilizes a relatively thick metal liner to contain the pressurized fluid or gas and to support from one third to one half of the internal pre-sure load of the vessel. The remainder of the load is carried by the composite overwrap.

The composite pressure vessels with load sharing liners are intermediate in weight saving performance between thin metal/bonded liner composite vessels and homogeneous metal vessels, and do not require a bond between the metal shell and overwrap.

For vessels with load sharing liners, the filament stress strain curve is linearly elastic out to the proof strain and even beyond to burst. However, on the first pressurization (proof) cycle of the vessel, the metal liner is plastically strained while the composite overwrap is strained elastically.

As shown in Figure 11, the metal stress strain curve shows yield and plastic flow. Since this initial (proof) pressure cycle plastically deforms or "sizes" the liner, it is referred to as the "sizing" or "autofrettage" cycle. As the vessel proof pressure is released, the liner, which has taken a permanent plastic set, is forced into compression by the filaments trying to return elastically to their original size. Thus, at zero pressure after proof, the metal is in compression and the filament in tension.

From that time on, the metal operates elastically from compression to tension while the filaments operate in a tension mode when operating pressure is applied to the vessel.

The overwrapped load sharing liner concept has proven to be an efficient design for attainment of significant weight savings (40 percent) over the best all titanium pressure vessel design used in aerospace applications [6].

A Kevlar 49/epoxy composite pressure vessel equipped with a cryoformed 301 stainless steel load bearing liner achieved a P_bV/W of 2.1×10^4 meters compared to 1.5×10^4 meters for a titanium pressure vessels of similar shape, contained volume and pressure rating of 2000 N/cm^2 [6].

The load sharing lined composite vessels concept is currently utilized for high pressure gas containment vessels on the shuttle oribter, escape chute inflation pressure vessels on some commercial aircraft and for fire fighter's and suber diver's air breathing pressure vessels.

3.2 Pressure Vessels Fabrications

3.2.1 Filament Winding Layer

Pressure vessels are normally fabricated by the filament winding method. This method owes its origins to the textile industry and consists of winding continuous high strength/stiffness resin impregnated, or resin soaked fiber around a shaped mandrel, to some pre-specified winding pattern. Fiber windings and mandrel are subsequently autoclaved to cure the resin system, where upon the mandrel is removed to yield a high strength fiber composite shell.

The method is particularly suited to the manufacture of axisymmetric structure such as pressure vessels. A significant advantage of this method lies in the fact that it can be almost entirely automated and should thereby eliminate many of the manufacturing induced material inconsistencies that seem to plague "hand laid" fiber composite components.

Types of filament winding machine are many and varied but they basically fall into two categories which will be called 'helical winding' and 'polar winding' machines. The former simulate the action of the lathe with the mandrel in a horizontal position. The mandrel rotates and the fiber dispensing head traverses back and forth along its length dispensing fibers at a helix angle dependent upon the ratio between traversing and rotational velocities. A variant of this type of machine locates the mandrel in a vertical axis, which reduces mandrel body forces and gives better results when winding large and heavy components. In the polar winding machines the fiber dispensing head is located at the end of a rotating arm, which passes over the forward and aft poles of the mandrel, while the mandrel itself rotates. This type of machine proves to be more efficient in the winding of end closures and has obvious advantages where it is required to lay fibers at a helix angle approximating to the longitudinal axis of the mandrel.

Both types of machine possess a facility for the application of fibers in a circumferential, or hoop direction.

3.2.2 Liner Fabrication

Aluminum liners for composite cylinders can be fabricated by impact extrusion. This is a two step process. First is an impact to make an open cup, and second is an impact on the open end of the cup to close it and form the boss.

Deep Draw and Spin

This is a multi-step operation with intermediate anneals. The final step is spin closing without a mandrel. Although more expensive than impact extrusion, this process permits thin wall liners with close tolerances on thicknesses. Normally aluminum liners 6061 or 6451 are heat treated to the T6 condition and then machined to shape the boss and provide threads for the valve.

Overwrap

The liner is completely filament wound with fibers in resin using interspersed helical and hoop patterns as previously described.

After overwrapping, a polyurethane coating of the desired color is applied to the cylinder and it is cured in an oven at about 150°C.

One problem area in the fabrication of composite structures is residual stresses due to thermal expansion mismatch between the composite and the tooling. Cost reduction is becoming a major concern in fabrication of structures, hence, it is desirable to eliminate all unnecessary steps. There is growing interest in using techniques as microwave and ultraviolet curing which is expected to shorten cure cycles [2].

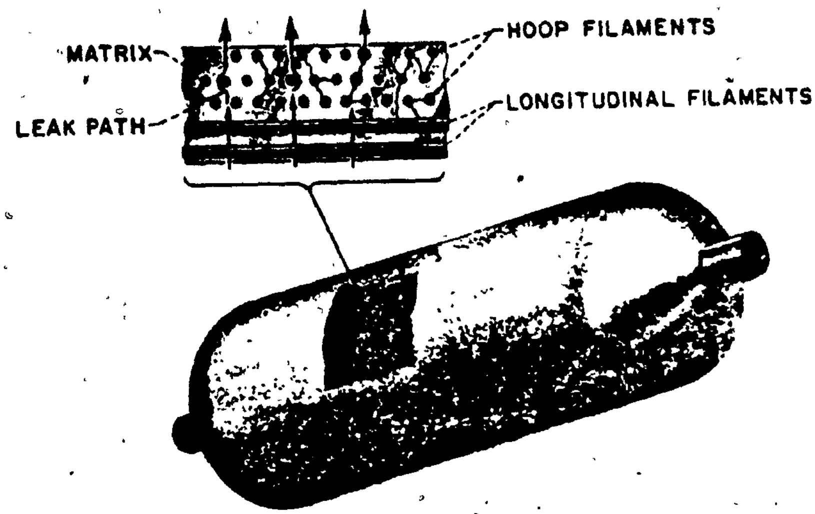

Figure 3 - Fiber/resin filament-wound composite pressure vessel. [6]

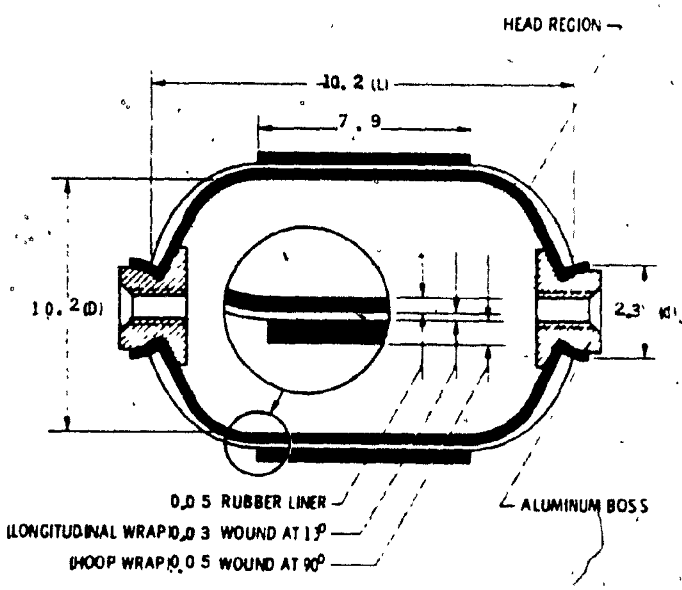

Fig.4-Design of the 10.2 cm diameter composite pressure vessel. [6]

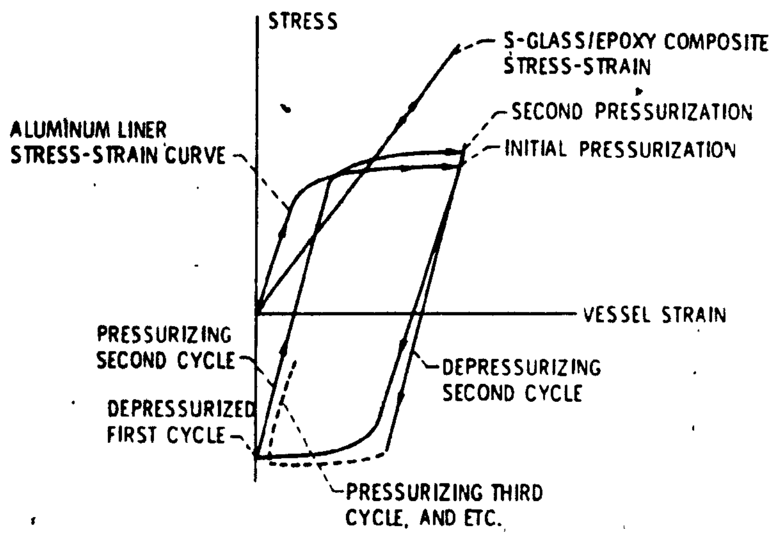

Figure 5 - Typical stress-strain plot for a filament-wound glass fiber/epoxy composite pressure vessel equipped with an adhesively-bonded thin aluminum liner. [6]

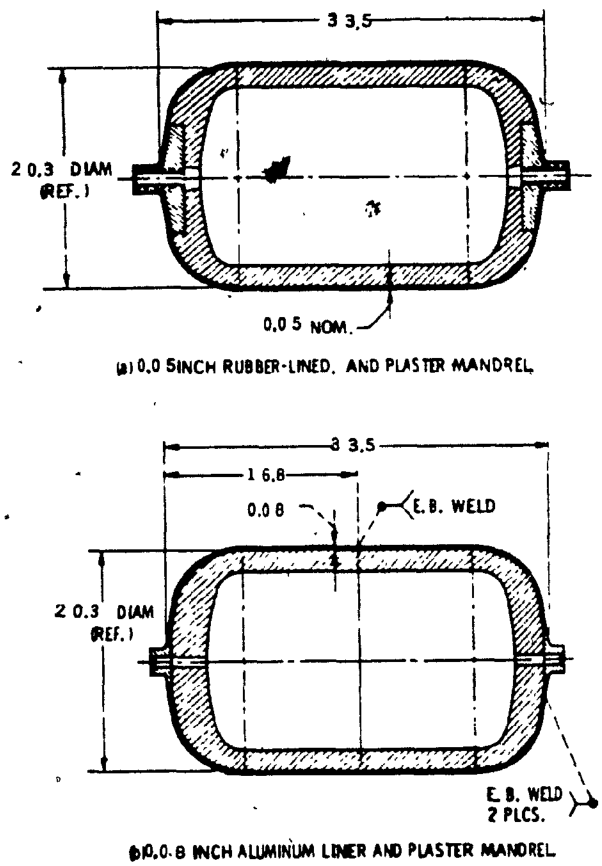

Fig.6-Liner designs for 20.3 cm diameter cylindrical composite pressure vessels. [6]

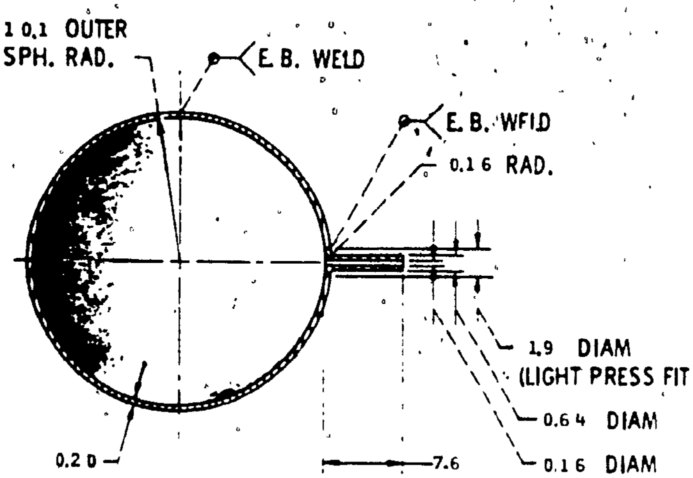

(a) SINGLE-BOSS SPHERICAL ALUMINUM LINER

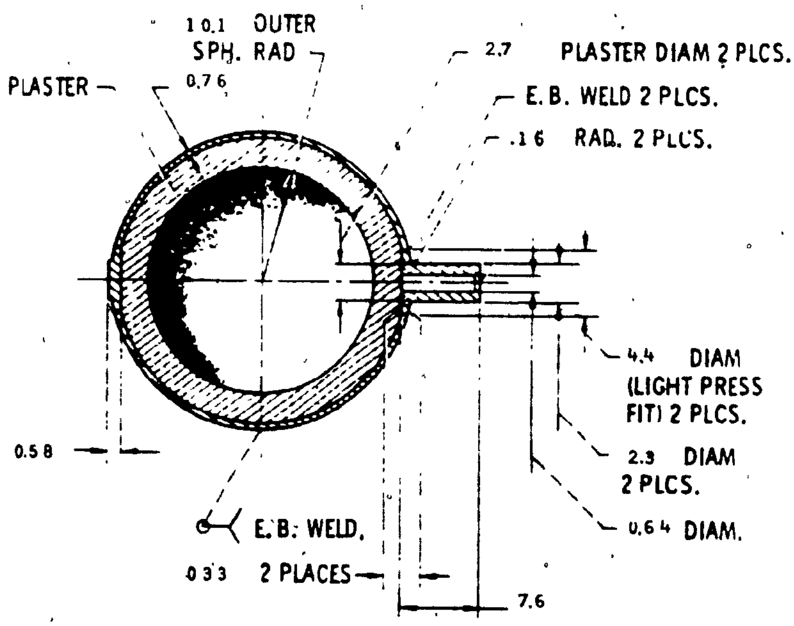

(b) DOUBLE-BOSS SPHERICAL ALUMINUM LINER.

Figure 7 - Liner designs for 20.3 cm diameter spherical composite pressure vessels. [6]

Figure 8

Interleaved Composite Pattern [1]

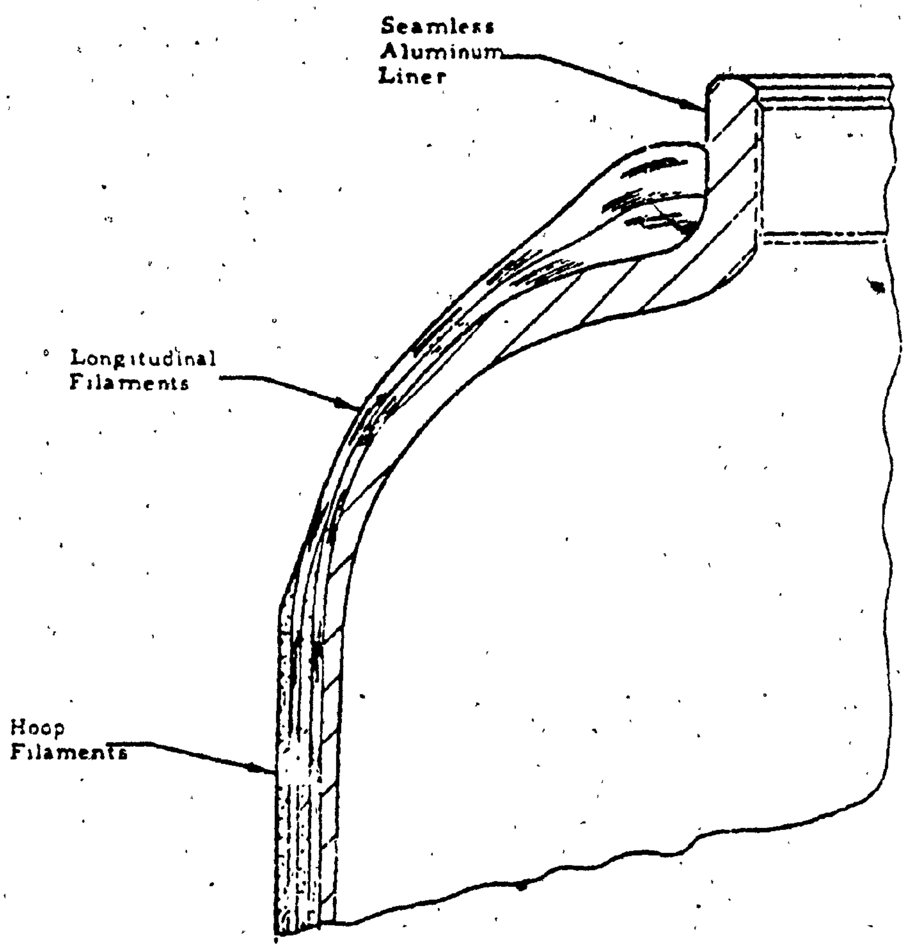

Figure 9

Some Material Effects On Weight And Cost Of Composite Compressed Gas Cylinders [1]

Filament	Metal / Material Characteristics	6061-T62 Aluminum	4130 Steel	Stainless Steel	
		• High Strength/Weight • Low Cost • Good Stress Corrosion Resistance • Good Fracture Toughness	• Moderate Strength/Weight • Moderate Cost • Poor Stress Corrosion Resistance • Good Fracture Toughness	• Moderate Strength/Weight • High Cost • Good Stress Corrosion Resistance • Good Fracture Toughness	Equivalent (1)
Kevlar -49	• High Strength/Weight • High Cost • 20% Organic	50	58	54	Weight
		250	250	270	Cost
S-2 Glass	• Moderate Strength/Weight • Low Cost • 7% Organic	63	70	67	Weight
		200	200	230	Cost

(1) Values given are a percentage of an equivalent 3AA or 3HT DOT Specification Cylinder

FIGURE 10

FIREMAN'S AIR BREATHING APPARATUS TANKS [1]

CURRENT STEEL PRESSURE VESSELS			GLASS FILAMENT WOUND ALUMINUM LINER	
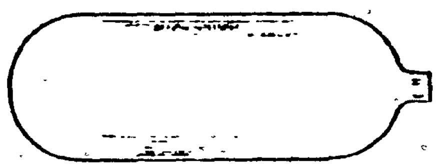			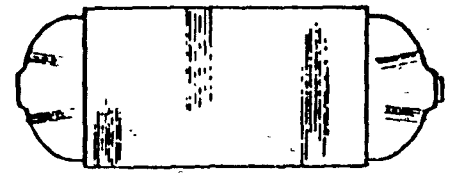	
1275 ℓ	1700 ℓ	CAPACITY	1700 ℓ	1275 ℓ
1528 N/cm^2	2069 N/cm^2	PRESSURE	2758 N/cm^2	1528 N/cm^2
30	40	DURATION, MIN	40	30
8.2 kg	12.1 kg	WEIGHT, EMPTY	6.4 kg	4.5 kg
10.3 kg	14.7 kg	WEIGHT, FULL & VALVE	9.0 kg	6.9 kg
		ADDITIONAL FEATURES	NON-RUSTING ALUMINUM LINER	

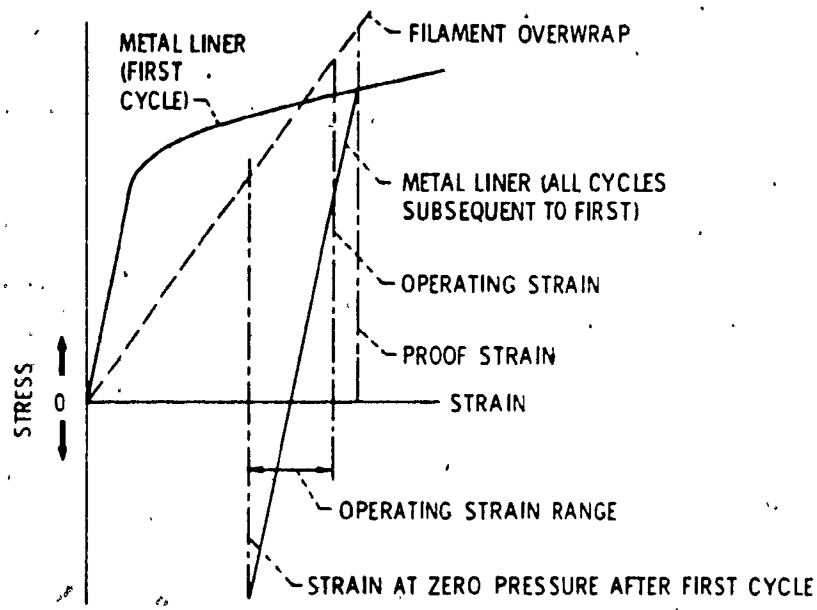

Figure 11- Typical stress-strain plot for a filament-wound S-glass fiber/epoxy composite pressure vessel equipped with a metallic load-bearing liner. [6]

Table 10 Test Results of Rubber-Lined 10.2 Diameter Kevlar 49/Epoxy Composite Pressure Vessels [6]

	Control[a]	L/D ratios		d/D ratios		Dome contours	
	1	2	3	4	5	6	7[b]
Vessel design							
Dome contour	In-plane	In-plane	In-plane	In-plane	In-plane	Helical	Hemispherical
Boss/diameter, d/D	0.23	0.23	0.23	0.10	0.17	0.10	0.10
Length/diameter, L/D	1.38	2.00	3.00	1.38	1.38	1.38	1.38
Single-cycle burst pressure,[c] P_b							
Mean, $10^6\ N/m^2$	18.6	17.8	17.1	17.2	19.1	17.1	6.1
Failure location[d]	17H-4F	6H-1K	3H-2K	9H	7H-1K	5H-4K	1H (equator)
Composite modulus at failure $10^9\ N/m^2$							
Longitudinal	33.1	33.8	35.9	34.5	34.5	34.5	34.5
Hoop	56.5	53.8	45.5	57.9	57.9	56.5	51.7
Rupture strain, %							
Axial	1.7	1.6	1.5	1.7	1.7	1.5	0.5
Hoop	2.0	2.0	1.5	2.0	2.0	1.9	0.7
Weight of composite, KG	0.05	0.07	0.10	0.05	0.05	0.05	0.05
Volume of vessels, $10^{-3}\ m^3$	0.94	1.4	2.2	0.92	0.92	0.93	1.1
$P_b V/W$, 10^6 cm composite, mean	4.0	3.8	3.9	3.9	4.0	4.6	1.4
Fiber content, by volume %	67.5	66.7	69.1	68.0	66.7	65.9	66.3
Density $10^3\ KG/m^3$	1.4	1.4	1.4	1.4	1.4	1.4	1.4
Vessel thickness, cm	0.08	0.08	0.08	0.08	0.08	0.08	0.08
Longitudinal winding	0.03	0.03	0.03	0.03	0.03	0.03	0.03
Hoop winding	0.05	0.05	0.05	0.05	0.05	0.05	0.05
Calculated fiber hoop failure stress, $10^6\ N/m^2$ mean	2944	2889	2668	2986	2386	2758	903

[a] Standard 10.2 cm diameter model vessels

[b] One vessel only.

[c] Tested at ambient temperature

[d] Nominal failure locations are (1) H for hoop, K for knuckle, and F for fitting; thus 2H and 1K indicate two vessels failed in hoop and one in knuckle. Note - the number preceding the letter indicates the number of vessels tested

Table 11 Extensibility of Vessel and Liner Materials [6]

Materials	Maximum elastic strain, per cent[a]	
	Test temperature	
	25° C	253° C
S-glass epoxy	3.5	3.8
Kevlar 49/epoxy	2.5	N/A
Thornel-Special graphite/epoxy	1.7	N/A
Thornel 400 graphite/epoxy	1.6	N/A
Elastomers	700	0
Aluminum (maximum elastic strain)	.07	.1
Titanium (6Al-4V), annealed (maximum elastic strain)	.6	N/A

[a]Based on fracture strain.

Table 12 Test Results of Cylindrical Aluminum-Lined[a] 20.3 cm Diameter Kevlar 49/Epoxy Composite Pressure Vessels [6]

(Test temperature, 25°C)

Vessel test results						
Vessel number	P-143	P-145	P-147	P-149	P-177	P-180
Volume, 10^{-3} m^3	9.22					
Single cycle burst pressure, N/m^2	14.34	14.7	14.0	17.1	15.2	14.2
Failure location[b]	H	H	F	H	F	H
P_bV/W, 10^6 cm composite	3.6	3.8	3.6	4.5	4.1	4.0
Composite data						
Total wall thickness, cm	0.14	0.14	0.14	0.14	0.14	0.14
Longitudinal wrap, cm	0.61	0.61	0.61	0.61	0.61	0.61
Hoop wrap, cm	0.86	0.86	0.86	0.86	0.86	0.86
Weight, KG	0.38	0.36	0.37	0.36	0.35	0.34
Fiber content, vol %	76.5	69.9	68.6	70.3	71.3	69.7
Calculated fiber stress, 10^6 N/m^2						
Hoop wrap	2496	2530	2427	2950	2827	2586
Axial	2978	2282	2660	2864	2317	2213

[a] 0.030-inch thick liner

[b] H for hoop, F for fitting.

Table 13 Test Results of Spherical 20.3 cm Diameter Kevlar 49 Epoxy Composite Pressure Vessels [6]

Vessel properties			
Liner	Aluminum (0.08)	Aluminum (0.08)	Rubber[a]
Boss type	Large double	Small single	Small single
Number of vessels	10	6	4
Volume, m^3	--	4.07	--
Composite wall thickness, cm at equator	0.22	0.21	0.22
Composite weight, KG	0.35	0.34	0.36
Fiber content, vol.%	69.9	67.9	68.1
Test data			
Single cycle burst pressure, mean, ksi	28.75	[b] 38.95	35.44
P_bV/W, 10^6 cm composite, mean	3.4	[c] 4.2	4.1

[a] Rubber liner over perforated aluminum.

[b] Strength contribution of liner not considered in calculations.

[c] Data corrected for liner strength contribution.

CHAPTER (4)

STRUCTURAL AYALYSIS

4.1 Laminate Theory

Laminates suited to pressure vessel structure will usually require bidirectional strength, necessitating at least two orientations of fibre layup (two fiber system). It is likely however, that a multitude of differing fibre winds will satisfy any given design criterion and means of identifying and quantifying these design variations form the main topic of this section.

Limitations as to the number of varying fibre orientations allowed in any given design must be specified. The more fibre orientations that are introduced, the more complicated and expensive will be the manufacturing process and it is thought that a three fibre system provides the right compromise between variability of design and ease of production.

The three fibre system will comprise 'angle ply', i.e. fibres orientated alternately at plus and minus θ° to a reference direction and 'hoop' or 'circumferential' ply, which is all aligned in the hoop direction. Figure 12a shows filament winding patterns.

The complete structural configuration can be identified by two design variables, namely (R) and (θ), in which (R) specified the percentage of total laminate thickness committed to angle ply and (θ) the angle, (plus and minus alternately) of angle ply [7].

A layup specified by R = 0.4 and $\theta = 20^{\circ}$ would therefore comprise 20% of its thickness oriented at 20°, 20% at -20° and 60% hoop ($\theta = 90^{\circ}$).

Figure 12b illustrates the layup of the example.

Vessel Coordinate System

The cylindrical shell structure is described by an orthogonal (x, y, z) curvilinear axis system, so that z = 0 defines a reference surface within the shell thickness and x and y align with axial and circumferential directions respectively to complete a right handed system (see Figure 13). [8]

4.1.1 Laminate Elastic Constant Prediction

In general the only measured material properties available to the designer are those referring to the unidirectional layer.

Structural laminates are however (as implied above) normally composed of a number of unidirectional layers, whose fibres are orientated at differing angles relative to a given reference direction. Each laminate will therefore possess different overall elastic constants depending on the particular stacking sequence employed and methods must be readily available for obtaining these elastic constants from constituent unidirectional data.

This section is primarily concerned with the membrane analysis of thin laminates. The only elastic constants of relevance in this section are therefore those referring to the plane of the laminate.

Material Coordinate System

The unidirectional lamina is identified by an orthogonal (1, 2, 3) axis system so that direction (1) aligns with the fibres and directions (2) and (3) are at right angles to the fibres, forming a right handed system, (see Figure 14a). The (1, 2, 3) axis system is transformed to the global (x, y, z) axis system via a rotation (θ) about the (3, z) axis (see Figure 14b).

Unidirectional Stress - Strain Relationships [9, 10]

Assuming orthotropic symmetry and transverse isotropy.

Generalized Hooke's Law

If it is assumed that the relationship between stresses and strains is linear, then the following equations must exist to describe the behaviour of an anisotropic material.

$$\begin{Bmatrix} \varepsilon_{11} \\ \varepsilon_{22} \\ \varepsilon_{33} \\ \gamma_{13} \\ \gamma_{23} \\ \gamma_{12} \end{Bmatrix} = \begin{bmatrix} S_{11} & S_{12} & S_{13} & S_{14} & S_{15} & S_{16} \\ S_{21} & S_{22} & S_{23} & S_{24} & S_{25} & S_{26} \\ S_{31} & S_{32} & S_{33} & S_{34} & S_{35} & S_{36} \\ S_{41} & S_{42} & S_{43} & S_{44} & S_{45} & S_{46} \\ S_{51} & S_{52} & S_{53} & S_{54} & S_{55} & S_{56} \\ S_{61} & S_{62} & S_{63} & S_{64} & S_{65} & S_{66} \end{bmatrix} \begin{Bmatrix} \sigma_{11} \\ \sigma_{22} \\ \sigma_{33} \\ \tau_{13} \\ \tau_{23} \\ \tau_{12} \end{Bmatrix} \qquad (1)$$

Where the matrix $\left[S\right]$ is termed the material compliance matrix.

$\left[S\right]$ is symmetrical and therefore 21 independent elastic constants are required to describe the fully anisotropic material.

<u>Orthotropic Symmetry</u>

If a material possesses three mutually perpendicular planes of elastic symmetry then it is said to be orthotropic and equations (1) are modified to the following.

$$\begin{Bmatrix} \varepsilon_{11} \\ \varepsilon_{22} \\ \varepsilon_{33} \\ \varepsilon_{13} \\ \varepsilon_{23} \\ \varepsilon_{12} \end{Bmatrix} = \begin{bmatrix} S_{11} & S_{12} & S_{13} & 0 & 0 & 0 \\ S_{12} & S_{22} & S_{23} & 0 & 0 & 0 \\ S_{13} & S_{23} & S_{33} & 0 & 0 & 0 \\ 0 & 0 & 0 & S_{44} & 0 & 0 \\ 0 & 0 & 0 & 0 & S_{55} & 0 \\ 0 & 0 & 0 & 0 & 0 & S_{66} \end{bmatrix} \begin{Bmatrix} \sigma_{11} \\ \sigma_{22} \\ \sigma_{33} \\ \tau_{13} \\ \tau_{23} \\ \tau_{12} \end{Bmatrix} \qquad (2)$$

$[S]$ is still symmetric and therefore materials posssessing orthotropic symmetry only require the definition of 9 independent elastic constants.

Transverse Isotropy

If an addition to orthotropic symmetry a material contains a plane where its elastic relationships are constant in all directions then this material is termed 'transversely isotropic'. If the 2, z plane is the plane of isotropy then equation (2) becomes:

$$\begin{vmatrix} \varepsilon_{11} \\ \varepsilon_{22} \\ \varepsilon_{33} \\ \varepsilon_{13} \\ \varepsilon_{23} \\ \varepsilon_{12} \end{vmatrix} = \begin{bmatrix} S_{11} & S_{12} & S_{12} & 0 & 0 & 0 \\ S_{12} & S_{22} & S_{23} & 0 & 0 & 0 \\ S_{12} & S_{12} & S_{22} & 0 & 0 & 0 \\ 0 & 0 & 0 & S_{44} & 0 & 0 \\ 0 & 0 & 0 & 0 & S_{55} & 0 \\ 0 & 0 & 0 & 0 & 0 & S_{44} \end{bmatrix} \begin{vmatrix} \sigma_{11} \\ \sigma_{22} \\ \sigma_{33} \\ \sigma_{13} \\ \sigma_{23} \\ \sigma_{12} \end{vmatrix} \qquad (3)$$

S_{55} is no longer independent and is related to S_{22} and S_{23} so that now only 5 independent constants are required to describe the material.

Then the stress strain relationships for a unidirectional layer become:

$$\varepsilon_{11} = \frac{1}{E_{11}}\left[\sigma_{11} - \mu_{12} \quad \sigma_{22} - \mu_{12} \quad \sigma_{33}\right]$$

$$\varepsilon_{22} = \frac{1}{E_{22}}\left[\frac{-\mu_{12}E_{22}}{E_{11}} \quad \sigma_{11} + \sigma_{22} - \mu_{23} \quad \sigma_{23}\right] \qquad (4)$$

$$\varepsilon_{33} = \frac{1}{E_{22}}\left[\frac{-\mu_{12}E_{22}}{E_{11}} \quad \sigma_{11} - \mu_{23} \quad \sigma_{23} + \sigma_{33}\right]$$

$$\gamma_{23} = \tau_{23} \Big/ \frac{E_{22}}{2(1 + \mu_{23})}$$

$$\gamma_{13} = \tau_{31}/G_{12}$$

$$\gamma_{12} = \tau_{12}/G_{12}$$

Or in matrix form

$$|\varepsilon|_{123} = [S]^{L}_{123} \quad |\sigma|_{123} \qquad (5)$$

Where $[S]^{L}_{123}$ is termed the local compliance matrix, the suffix (L) signifying 'layer'

Axis Rotation

The stress vector $|\sigma|_{123}$ and strain vector $|\varepsilon|_{123}$ can be referred to the (x, y, z) axis system via the following relationships:

$$|\varepsilon|_{xyz} = [T]\,|\varepsilon|_{123}$$
$$|\sigma|_{123} = [T]^T|\sigma|_{xyz} \qquad (6)$$

Where the suffix 'T' denotes transpose and the rotation matrix $[T]$ is that conductive to a rotation (θ) about the 3 axis

$$[T]=\begin{bmatrix} m^2 & n^2 & 0 & 0 & 0 & mn \\ n^2 & m^2 & 0 & 0 & 0 & -mn \\ 0 & 0 & 1 & 0 & 0 & 0 \\ 0 & 0 & 0 & m & -n & 0 \\ 0 & 0 & 0 & n & m & 0 \\ -2mn & 2mn & 0 & 0 & 0 & (m^2-n^2) \end{bmatrix}$$

Where $m = \cos\theta$ $\quad n = \sin\theta$

From (5) and (6)

$$|\varepsilon|^L_{xyz} = [T]^L |S|^L_{123} \left([T]^T\right)^L \; |\sigma|^L_{xyz}$$

or

$$|\varepsilon|^L_{xyz} = [S]^L_{xyz} \; |\sigma|^L_{xyz} \qquad (7)$$

Where $[S]^L_{xyz}$ is the global compliance matrix for the layer

From (7)

$$|\sigma|^L_{xyz} = [C]^L_{xyz} \; |\varepsilon|^L_{xyz} \qquad (8)$$

Where $[C]^L_{xyz} = \left([S]^L_{xyz}\right)^{-1}$ is the global material stiffness matrix for the layer.

Lamina Stress Resultant

From Eq. (8) the stress resultants acting in a single layer must be given by:

$$|N|^L_{xyz} = t_L \; [C]^L_{xyz} \; |\varepsilon|^L_{xyz} \qquad (9)$$

Where t_L is the thickness of the layer

Laminate Stresses

From Eq. (9) the average laminate stresses must be given by:

$$|\sigma|^{Lt}_{xyz} = \sum_{L=1}^{K} \left[\left(t_L / T \right) [C]^L_{xyz} \; |\varepsilon|^L_{xyz} \right] \qquad (10)$$

Where (K) is the total number of layers in the laminate and (T) is the total laminate thickness. The suffix Lt refers to total laminate properties.

Let laminate and lamina strains be equal, then

$$|\varepsilon|_{xyz}^{L} = |\varepsilon|_{xyz}^{Lt} \tag{11}$$

and eq.(10) becomes

$$|\sigma|_{xyz}^{Lt} = [B]\ |\varepsilon|_{xyz}^{Lt} \tag{12}$$

where

$$[B] = \sum_{L=1}^{K} \left(t_L / T\right)[C]_{xyz}^{L}$$

<u>In Plane Elastic Constants</u>

From eq.(12)

$$|\varepsilon|_{xyz}^{Lt} = [A]\ |\sigma|_{xyz}^{Lt} \tag{13}$$

where $|A| = [B]^{-1}$

The stress-strain relationships for the assembled laminate will be of the following form: -

$$
\begin{aligned}
\varepsilon_{xx} &= \frac{1}{E_{xx}}\left[\sigma_{xx} - \mu_{xy}\,\sigma_{yy} - \mu_{xz}\,\sigma_{zz}\right] \\
\varepsilon_{yy} &= \frac{1}{E_{yy}}\left[-\mu_{yx}\,\sigma_{xx} + \sigma_{yy} - \mu_{yz}\,\sigma_{zz}\right] \\
\varepsilon_{zz} &= \frac{1}{E_{zz}}\left[-\mu_{zx}\,\sigma_{xx} - \mu_{zy}\,\sigma_{yy} + \sigma_{zz}\right] \\
\gamma_{yz} &= \tau_{yz} / G_{yz} \\
\gamma_{xz} &= \tau_{xz} / G_{xz} \\
\gamma_{xy} &= \tau_{xy} / G_{xy}
\end{aligned}
\qquad (14)
$$

Comparing equations (13) with equations (14) yields the following expressions for the elastic constants of the assembled laminate in the plane of the laminate.

$$
\begin{aligned}
E_{xx} &= {}^{1}/A_{11} \qquad & E_{yy} &= {}^{1}/A_{22} \\
\mu_{xy} &= A_{12}/A_{11} \qquad & \mu_{yx} &= A_{21}/A_{22} \\
G_{xy} &= {}^{1}/A_{66}
\end{aligned}
\qquad (15)
$$

Transverse Shear Moduli

The condition of constant laminate - lamina strain (Eq.(11) is only realistic for the in plane strains ε_{xx}, ε_{yy} and γ_{xy} and the following expressions can therefore only be regarded as approximations to the transverse shear moduli.

Once more comparing equations (13) with equations (14)

$$G_{yx} = {}^{1}/A_{44} \qquad G_{xz} = {}^{1}/A_{55} \qquad (16)$$

Example for the Derivation of Elastic Constants for Angle Plied Laminate)

Following is a derivation of the elastic constants for an angle plied block of a carbon fiber reinforced plastic (C.F.R.P.) Type I material which its unidirectional fiber properties are shown in Table 14. As the fibre angle may be varied from $\pm 0^\circ$, (i.e. all fibres align in the 'X' direction) to $\pm 90^\circ$ (i.e. all fibres aligned in the 'Y' direction), using equation 15 the results of this analysis are plotted in Figure 15 and 16 which respectively show the variation with ply angle ($\pm\theta$) of the three Young's moduli and the six Poisson's ratios.

The moduli plot, Figure 15, shows that the out-of plane Young's modulus Ez, is independent of fibre orientation, which is as expected as this is always a transverse property and as such must be primarily resin dependent.

In plane moduli Ex and Ey decrease and increase respectively as the angle of ply is increased from $\pm 0^\circ$.

The plot of Poisson's ratios Figure 16 shows that effective in plane Poisson's ratios μ_{xy} and μ_{yx} can exceed 2.0 for angle plied laminates. This is more a feature of geometry than of pure elasticity and is best appreciated by considering the analogy of a four bar chain (see Figure 17). It can be seen from this figure that when such a mechanism is sheared to a fairly acute angle, a small extension of its longitudinal axis (x) can result in a significantly magnified contraction of its transverse axis (y).

4.1.2 Laminate Strength Prediction

In the previous section it was shown how the process of lamination facilitates the assembly of a virtually unlimited range of physically differing materials from the same unidirectional fibre - matrix building block. The range of possible material variants is so large, as to make the experimental collation of strength data on assembled laminates completely impracticable. Methods similar to those used for elastic constants prediction must therefore be made available, whereby the strength of an assembled laminate can be assessed from the measured strength data of a single constituent layer.

Experimental strength data are best related to uniaxial stress systems, such as those resulting from the simple tensile, compressive and shear testing of a unidirectional layer. In service however, layers will undoubtedly be subjected to simultaneously applied longitudinal, transverse and shear stresses.

The method of laminate strength prediction must therefore be capable of relating this complex multi axial state of stress to the simple uniaxially measured strength data.

Failure Criterion

Numerous failure criteria have been suggested for application to filamentary materials, including minimum and maximum stress theories and even statistical theories based on probability theory. Most researchers in this field however agreed that distortional energy theories give the most encouraging results [10, 11] and such a theory originated by Tsai [10] and modified by Hill [11] will be used in this study. This method basically consists of equating the energy of distortion of a block of material subjected to a multiple stress system, to the energy required to cause yielding, or failure in a simple tensile test.

Generalising the Von Mises yield criterion for isotropic materials to include the effects of anisotropy, Hill (15) assumed a quadratic in the stress components, i.e.

$$(G + H)\ \sigma_{11}^2 + (F + H)\ \sigma_{22}^2 + (F + G)\ \sigma_{33}^2 - 2H\sigma_{11}\sigma_{22} - 2G\sigma_{11}\sigma_{33}$$

$$- 2F\sigma_{22}\sigma_{33} + 2L\tau_{23}^2 + 2M\tau_{13}^2 + 2N\tau_{12}^2 = 1 \qquad (17)$$

Where F, G, H, L, M, N are material anisotropic coefficients.

Let the only non zero stress acting be the limiting shear stress τ_{12} i.e. $(\tau_{12})L$, then from (17)

$$2N = \frac{1}{(\tau_{12}^2)_L}$$

similarly

$$2M = \frac{1}{(\tau_{13}^2)_L} \quad ; \quad 2L = \frac{1}{(\tau_{23}^2)_L}$$

Let the only non zero stress acting be the limiting value of the direct stress σ_{11} i.e., $(\sigma_{11})_L$, then

$$G + H = \frac{1}{(\sigma_{11}^2)_L} \qquad (18)$$

similarly

$$F + H = \frac{1}{(\sigma_{22}^2)_L} \qquad (19)$$

and

$$F + G = \frac{1}{(\sigma_{33}^2)_L} \qquad (20)$$

solving (18), (19) and (20) simultaneously for F, G and H yields:

$$2H = \frac{1}{(\sigma^2_{11})_L} + \frac{1}{(\sigma^2_{22})_L} - \frac{1}{(\sigma^2_{33})_L}$$

$$2G = \frac{1}{(\sigma^2_{11})_L} + \frac{1}{(\sigma^2_{33})_L} - \frac{1}{(\sigma^2_{22})_L} \qquad (21)$$

$$2F = \frac{1}{(\sigma^2_{22})_L} + \frac{1}{(\sigma^2_{33})_L} - \frac{1}{(\sigma^2_{11})_L}$$

Substituting for H, G, F, N, M, L in (17) and assuming transverse isotropy yields:

$$\frac{\sigma^2_{11}}{(\sigma^2_{11})_L} + \frac{\sigma^2_{22}}{(\sigma^2_{22})_L} + \frac{\sigma^2_{33}}{(\sigma^2_{33})_L} - \frac{\sigma_{11}\sigma_{22}}{(\sigma^2_{11})_L} - \frac{\sigma_{11}\sigma_{33}}{(\sigma^2_{11})_L}$$

$$- \left|\frac{2}{(\sigma^2_{22})_L} + \frac{1}{(\sigma^2_{11})_L}\right| \sigma_{22}\sigma_{33} + \frac{\tau^2_{23}}{(\tau^2_{23})_L} + \frac{\tau^2_{13}}{(\tau^2_{13})_L}$$

$$+ \frac{\tau^2_{12}}{(\tau^2_{12})_L} = 1 \qquad (22)$$

For two dimensional elasticity i.e. thin laminated plates $\sigma_{33} = \tau_{13} = \tau_{23} = 0$ and (22) reduces to

$$\frac{\sigma^2_{11}}{(\sigma^2_{11})_L} + \frac{\sigma^2_{22}}{(\sigma^2_{22})_L} - \frac{\sigma_{11}\sigma_{22}}{(\sigma^2_{11})_L} + \frac{\tau^2_{12}}{(\tau^2_{12})_L} = 1$$

and introducing a strength factor SF

$$\frac{\sigma^2_{11}}{(\sigma^2_{11})_L} + \frac{\sigma^2_{22}}{(\sigma^2_{22})_L} - \frac{\sigma_{11}\sigma_{22}}{(\sigma^2_{11})_L} + \frac{\tau^2_{12}}{(\tau^2_{12})_L} = \frac{1}{(SF)^2} \qquad (23)$$

Provided unidirectional strength data is known the failure criterion (equation 23) then permits a layer by layer strength evaluation to highlight the weakest layer and identify stress levels at the initiation of failure. Layer failures are indicated when the strength or reserve factor (SF) falls below unity.

Layer Stresses

Equations (22) and (23) refer exclusively to the unidirectional layer and therefore, restricting discussions to the two dimensional case, the laminate stress system σ_x, σ_y, τ_{xy} must be transformed to the local coordinate system of individual layers before any strength assessments can be made:

From equation (13)

$$\left|\varepsilon\right|^{Lt}_{xyz} = \left|\varepsilon\right|^{L}_{xyz} = \left[A\right]\left|\sigma\right|^{Lt}_{xyz} \qquad (24)$$

Multiplying both sides of (24) by $\left[C\right]^{L}_{xyz}$ yields

$$\left[C\right]^{L}_{xyz}\left|\varepsilon\right|^{L}_{xyz} = \left[C\right]^{L}_{xyz}\left[A\right]\left|\sigma\right|^{Lt}_{xyz}$$

Therefore from equation (8)

$$\left|\sigma\right|^{L}_{xyz} = \left[C\right]^{L}_{xyz}\left[A\right]\left|\sigma\right|^{Lt}_{xyz} \qquad (25)$$

Multiplying both sides of (25) by $\left[T\right]^{T}$ yields

$$\left[T\right]^{T}\left|\sigma\right|^{L}_{xyz} = \left[T\right]^{T}\left[C\right]^{L}_{xyz}\left[A\right]\left|\sigma\right|^{Lt}_{xyz}$$

therefore from equation (6)

$$\left|\sigma\right|^{L}_{123} = \left[T\right]^{T}\left[C\right]^{L}_{xyz}\left[A\right]\left|\sigma\right|^{Lt}_{xyz} \qquad (26)$$

The layer stress relationships (equation 26) allow the evaluation of stresses in the principal material directions (1, 2, 3) at each layer when the assembled laminate is subjected to orthogonal direct stress σ_x, σ_y and shear stress τ_{xy}. So these relationships are dependent on the applied stress system (σ_x, σ_y, τ_{xy}) and the fiber system (laminate layup) which in turn dependent on the design variables (R) and (θ). There are two stress systems applied to pressure vessels, the uni-axial tension, as may be experienced when there is pressurization with no longitudinal restraint such as pipe lines, and the second applied stress system of prime importance in this survey is the bi-directional stress system of cylindrical pressure vessels of the form shown in figure 12.

4.2 Design consideratios

The most common fiber systems in pressure vessels are the two and three fiber systems. For stress analysis there are also two different approaches. To verify the structural integrity of composite pressure vessels the continuum analysis approache gives resin strain as well as fiber strains and includes both fibers and resin strength data in the laminate failure criterion. The other approach is the netting analysis which ignores all resin effects so the structure is assumed sound until the actual breaking strain of the fibers is reached.

The following sections show the differences between two and three fiber systems and the derivation of elastic constant and strength characteristic for both systems.

Some useful relationships are derived for both two and three fiber systems by applying the bi-directional stress system (the applied stress system in cylindrical pressure vessels). Also the differences between continuum and netting analysis are explained followed by an example of a cylindrical pressure vessel (bi-directional applied stress system) using a two-fiber system to clarify the differences between continuum and netting analysis.

4.2.1 Three Fibre System

Three fiber system will comprise fibers orientated at plus and minus θ^{o} to a reference direction 'angle ply' and fibers aligned in the circumferential direction 'hoop ply'.

Elastic Constant Characteristics

Employing the design variables (R) and (θ) it is possible to specify the elastic constant characteristics in plane moduli E_x, E_y and G_{xy} over the whole design space R = 0.0 to 1.0 and $\theta = 0^{o}$ to 90^{o} by using equations 15. Such information can be organised in the form as shown in figures 19-21 for the carbon fiber reinforced plastic material which its unidrectional fiber properties are shown in table 14.

Strength Characteristics

In figures 22-24 strength characteristics are exhibited over the whole spectrum of 'in plane' applied stresses. While the structural laminate is held constant using the design variables (R) and (θ) this philosophy can be reversed so that the applied stress system remains constant whilst the actual laminate is varied. As it has been shown before the layer stress relationships (equation 26) are dependent on the applied stress system and the laminate lay up. So with the applied stress system held constant layer strength factors and subsequent laminate strength, based on the weakest layer, are therefore calculable from the failure criterion (equation 23) for any selective values of (R) and (θ). If (R) and (θ) are allowed to vary sequentially through the design space (i.e. R = 0 to 1.0, θ = 0 to 90°) strength data can be collated to cover all possible three fiber designs.

This process could easily be programmed to facilitate the production of strength design charts for any specific applied stress system. Such a program is developed in ref. [12].

4.2.2 Two Fiber System

The two fiber system configuration can be accomplished by having the design variable (R) set at unity which implies that all the material in the cross section in angle plied at ±θ degree. Which may be considered as a specific case of three fiber system. So the elastic constant and strength characteristics can be determined from figures 19-21 and 22-24 respectviely for a carbon fiber reinforced plastic which its unidirectional material properties as shown in table 14.

4.2.3 Bi-Directional Stress System

The applied stress system of the 2/1 ratio is the typical system of cylindrical pressure vessels of the form shown in Figure 18.

For this bi-directional stress system a laminate comprising at least two fiber orientations is required and the following useful relationships can be derived from netting analysis.

Considering first a two fiber system comprising a balanced helical angle ply with layers orientated at plus and minus θ^o to the hoop direction of the vessel.

From equilibrium:

$$\text{Hoop stress} = \sigma_h = \frac{PR}{t} = \sigma_1 \cos^2\theta$$
$$\text{Longitudinal stress} = \sigma_L = \frac{PR}{2t} = \sigma_1 \sin^2\theta \qquad (27)$$

Where σ_1 is the layer stress in the direction of fibers

Therefore from (27)

$$\frac{\sigma_h}{\sigma_L} = 2 = \frac{1}{\tan^2\theta} \qquad (28)$$

From which $\theta = 35.3^{\circ}$

For the three fiber system defined by (R) and (θ).

Where $\theta = 0$ refers to the hoop direction

$$\sigma_h = (1 - R)\,\sigma_{1h} + R\,\sigma_{1a}\cos^2\theta$$
$$\sigma_L = R\,\sigma_{1a}\sin^2\theta \qquad (29)$$

Where σ_{1h} is the stress in the direction of fibers for the hoop layers and σ_{1a} is the stress in the direction of fiber for the angle plies.

If $\sigma_{1h} = \sigma_{1a}$ and $\sigma_h/\sigma_L = 2$

equation (29) reduces to:

$$\frac{1 - R}{R} = 2\sin^2\theta - \cos^2\theta \qquad (30)$$

From (27) and (28)

$$\sigma_L = \sigma_{h/2} = \sigma_1 \ \text{Sin}^2 \ (35.26)$$

Therefore

$$\underline{\sigma_L = \sigma_{h/2} = 0.3334\sigma_1} \qquad (31)$$

A random solution to (30) is $\theta = \pm 70°$
$R = 0.3775$

and from (29)

$$\sigma_L = \sigma_{h/2} = 0.3775 \ \sigma_1 \ \text{Sin}^2 70 = \underline{0.3334\sigma_1} \qquad (32)$$

It can be seen that relationships (31) and (32) are identical and it can therefore be concluded that provided fiber stresses in all layers are equal, the two and three fiber system designs are of equal merit from a strength and hence weight point of view.

Relationship (32) was however derived from a random solution to Eq. (30) and an infinite number of such solutions are therefore possible offering an infinite number of differing designs of equal strength merit for the three fiber system, whilst only one solution exists for the two fiber system. (This is an important observation as it opens up possibilities of optimising the fiber layup to satisfy manufacturing constraints, or perhaps specific overall structure stiffness requirements).

Strength chart conducive to this stress system is shown in Figure 25.

4.2.4. Continuum - Netting Analysis

4.2.4.1 Continuum Analysis

Continuum theory assumes that the load reacted in a fiber/matrix composite is carried by both the fibers and resins simultaniously. So for design based on continuum analysis, laminate strengths are predicted from a yield type failure criterion (equation 23) involving the evaluation of the local stress system at a given layer and the measured longitudinal, transverse and shear (longitudinal - transverse plane) strengths of the uni-directional composite.

Since laminate strengths must depend on the applied stress system, it is possible to produce strength charts in terms of the design variables for specific load cases.

For the stress system of a simple pressure vessel, i.e. where the biaxial stress ratio (hoop to longitudinal) is 2.0 strength data are plotted in Figure 23, 24 for the same (R) & (θ) combinations. For these figures the dependent variable is chosen as the allowable hoop stress, which from simple calculations allows the pressure vessel wall thickness to be evaluated for any specific design, where the internal pressure is known.

4.2.4.2 Netting Analysis

Netting theory assumes that all load reacted in a fiber matrix composite is carried by the fibers and therefore, the only strength parameter of importance is that referred to the line of action of the fibers.

In producing netting analysis strength charts, the allowable material strength parameters used are therefore those listed in Table 14 for longitudinal tension.

For the pressure vessel load case where a bi-axial stress ratio of 2.0 is applied to the laminates, netting analysis results are a little more complex. Since stress is applied in two directions the angle plied layers can now carry a proportion of the load.

Strengths and stiffnesses in directions at right angles to the fibers must still be zero and the loads carried by the angle plied layers must therefore satisfy the strict geometry relationship. There must also be a strain compatibility between all layers in the laminate and for a three fiber system there are therefore sufficient equations to give solutions to stresses in each layer, for any combination of the design variables (R) and (θ). For any given value of the cross ply ratio (R), there will be a unique value of the angle ply angle (θ), to give constant stress in the fibers of all layers in the laminate. Designs specified in such a manner can be shown to be of minimum weight and therefore since (R) can be chosen as any value between 0.0 and 1.0, there will be an infinite number of optimum designs.

The allowable hoop stress (based on total shell thickness) is therefore directly related to the overall structure weight, and the higher this parameter, the lighter will be the final design. Strength data are plotted in figure 25.

An interesting design case is that where (R) is set at unity, which implies that all the material in the cross section is corss plied (i.e. two fibre system). For this case when, σ_x/σ_y is 2.0, the only cross ply angle satisfying netting analysis requirements is approximately $\theta = \pm 35.3^{\circ}$ to the hoop direction, as it has been derived before.

4.2 4.3 Netting - Continuum Strength Comparisons

For the applied stress system considered, it can be seen from figures 24 and 25 that there are significant differences between netting and continuum analysis results. Since, with netting analysis all resin effects are ignored, there can be no prediction of resin failure and the structure is assumed sound until the actual breaking strain of the fibers is reached (14,15).

Continuum analysis on the other hand, senses resin strain, as well as fiber strains and includes both fibers and resin strength data in the laminate failure criterion. Calculation procedurese of strength and stiffness using netting and continuum analysis are shown in a flow chart in Figure 26 [7].

For the pressure vessel load case large differences are apparent between netting and continuum analysis results. Taking the design for the two fiber system, (R = 1.0) from Figure 24 and 25, gives a maximum failing stress of approximately 217 Mn/m^2 for continuum analysis and 1270 Mn/m^2 for netting analysis, i.e. the continuum analysis strength prediction is almost a factor of six lower than the netting strength prediction.

The reason for these drastic differences in results can be best appreciated in considering a simple example.

4.3 EXAMPLE [16]

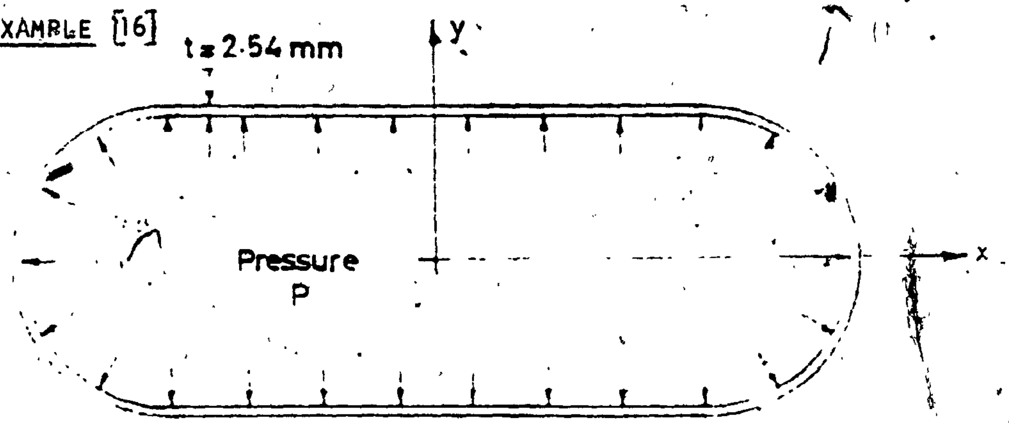

For the pressure vessel illustrated above, let the stress in the (x) direction σ_x be 34.5 MN/m^2 and that in the (y) direction σ_y be 69 MN/m^2 and let the design be a two fiber system in 3M G.F.R.P., at approximately 60% volume fraction

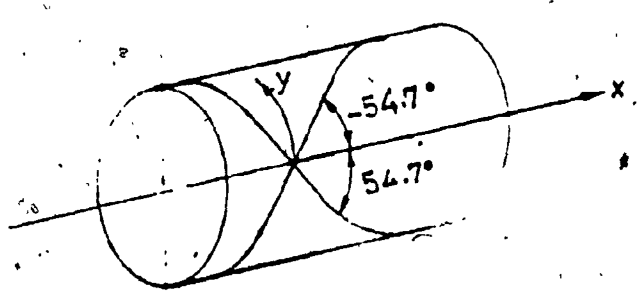

Since the example is a two fiber system, the only possible ply orientation for netting analysis is ±54.7° as indicated in the above sketch.

For netting analysis using equation 27

$$\sigma_1 = \frac{\sigma_y}{\sin^2 54.7} = \frac{69}{0.665} = 103.8 \text{ MN/m}^2$$

where σ_1 is the stress in the direction of the fibres.

From Table 14 the maximum longitudinal tensile stress for this material is 1904 MN/m^2.

Therefore the maximum allowable hoop stress is

$$69 \times \frac{1094}{103.8} = 1270 \text{ MN/m}^2$$

For input stress components σ_x = 34.5 MN/m^2 σ_y = 69 MN/m^2 and using the continuum analysis (equation 26) the stress systems in the l, t plane are:

Layers at + 54^o, σ_l = 85.6 MN/m^2, σ_t = 17.83 MN/m^2,
τ_{lt} = -7.12 MN/m^2

Layers at - 54^o σ_l = 85.6 MN/m^2, σ_t = 17.82 MN/m^2,
τ_{lt} = 7.12 MN/m^2

For continuum analysis the structural strength is specified from the 'Hill' criterion i.e. by using equation 23

$$\left(\frac{\sigma_l}{Q}\right)^2 - \frac{\sigma_l\,\sigma_t}{Q^2} + \left(\frac{\sigma_t}{R}\right)^2 + \left(\frac{\tau_{lt}}{S}\right)^2 = \frac{1}{F^2}$$

From Table 14 for 3M G.F.R.P.

$Q = 1904.0\ MN/m^2$, $R = 62.1\ MN/m^2$, $S = 68.2\ MN/m^2$

$$\frac{1}{F^2} = \left(\frac{85.6}{1904.0}\right)^2 - \frac{85.6 \times 17.82}{1904^2} + \left(\frac{17.82}{68.2}\right)^2 + \left(\frac{7.12}{68.2}\right)^2$$

$$\frac{1}{F^2} = 0.00202 - 0.00042 + 0.0822 + 0.0109$$

$$\therefore \frac{1}{F^2} = 0.1047 \quad \therefore \quad F = 3.1$$

∴ The maximum allowable hoop stress is

$69.0 \times 3.1 = 214\ MN/m^2$

From the above it can be seen that the first term of the left hand side of the Hill criterion is equivalent to netting analysis.

i.e: $\frac{\sigma_1}{Q} = \frac{1}{F}$ or $F = \frac{Q}{\sigma_1}$

The results show that σ_1 from continuum analysis, is of similar magnitude to the simple netting analysis value and therefore the components of the Hill criterion causing the difference between the two results (neglecting small term $\frac{\sigma_1 \sigma_t}{Q^2}$) are: -

$\left(\frac{\sigma_t}{R}\right)^2$ and $\left(\frac{\tau_{lt}}{S}\right)^2$

These two parameters refer primarily to the strength of the resin and since their magnitude in the Hill relationship is larger than the fibre term σ_l/Q, it is likely that resin failure is the limiting factor in continuum analysis results. By definition the transverse stress σ_t and the shear stress τ_{lt}, are zero for netting analysis and therefore no checks for resin failure can be made. As indicated previously netting analysis is therefore predicting an upper bound to the laminate strength, i.e. the point where fibre rupture must occur, but gives no information on the state of the resin. Continuum analysis on the other hand, predicts the point where failure of any nature takes place, including resin failure, which depending on the material may occur at stress levels far lower than those necessary to cause fibre rupture. In practice time dependence and non linearity of resin properties may also affect results. The material chosen for the above example is a glass fibre reinforced composite and it must be pointed out that differences between netting and continuum analysis are not as spectacular for the stiffer composites, i.e. Carbon, Boron.

4.4 Specifications and standards

For over sixty years, the commercial transportation of compressed gas has been restricted by the Depart of Transportation (DOT) to shipment in all metal cylinders, principally steel. As a practical matter, commercial compressed gas supply sources will not charge cylinders that do not have a DOT authorization. Thus, DOT authorization is essential for commercialization of composite pressure vessels technology.

The effort required to obtain the DOT authorization is an interesting case study of the difficulties involved in commercializing aerospace materials and process technology. The government "aerospace tanks" normally controlled by military specifications backed up by advanced analytical techniques and composite technology. However, on the other hand the commercial "compressed gas cylinders" backed with proven mechanical engineering practices going back to the 1930's.

Since the "proven mechanical engineering practices" control the issuance of the necessary DOT approvals, it was necessary to establish specifications for the composite materials and processes in terms that would assure DOT that cylinder fabricated of the materials would be as safe as the customary heavy steel ones.

There are codes and standards set forth by different agencies and government organizations to establish these specifications. Some of these requirements may be found in American Society of Mechanical Engineers (ASME) Boiler and Pressure Vessel Code Section 10 United States Department of Transport (DOT) Excemption DOT-E-8162 and Military Standard for Fiber Reinforced Plastics Pressure Vessel MIL-T-25363 [Ref. 14, 15, 16].

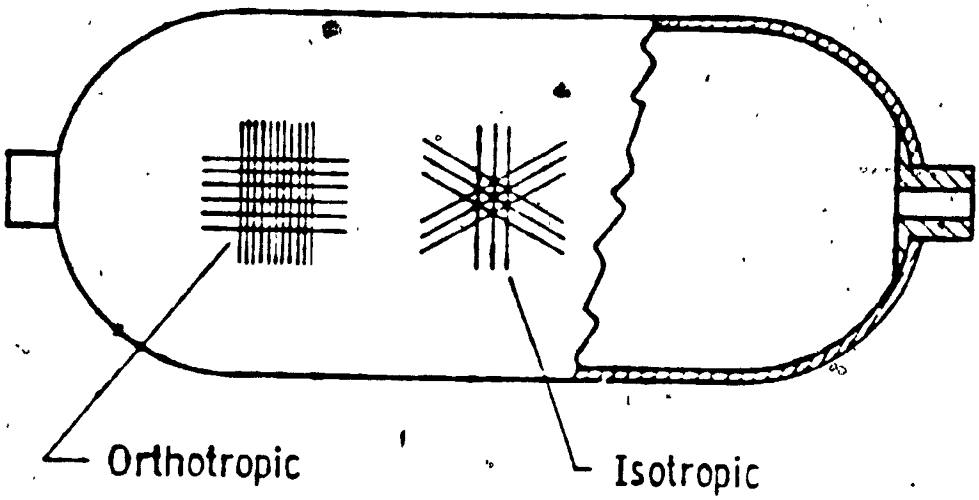

Figure 12 a Filament winding patterns

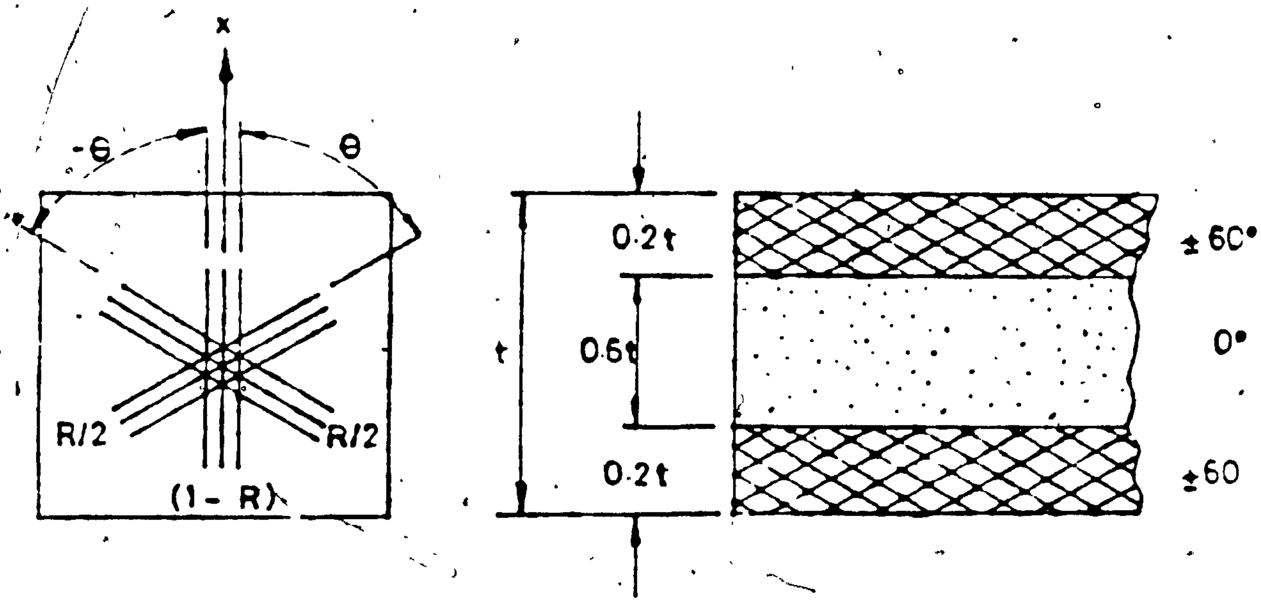

Fliament Winding Pattern
Figure 12b Specified by R = 0.4 and θ = 20° [13]

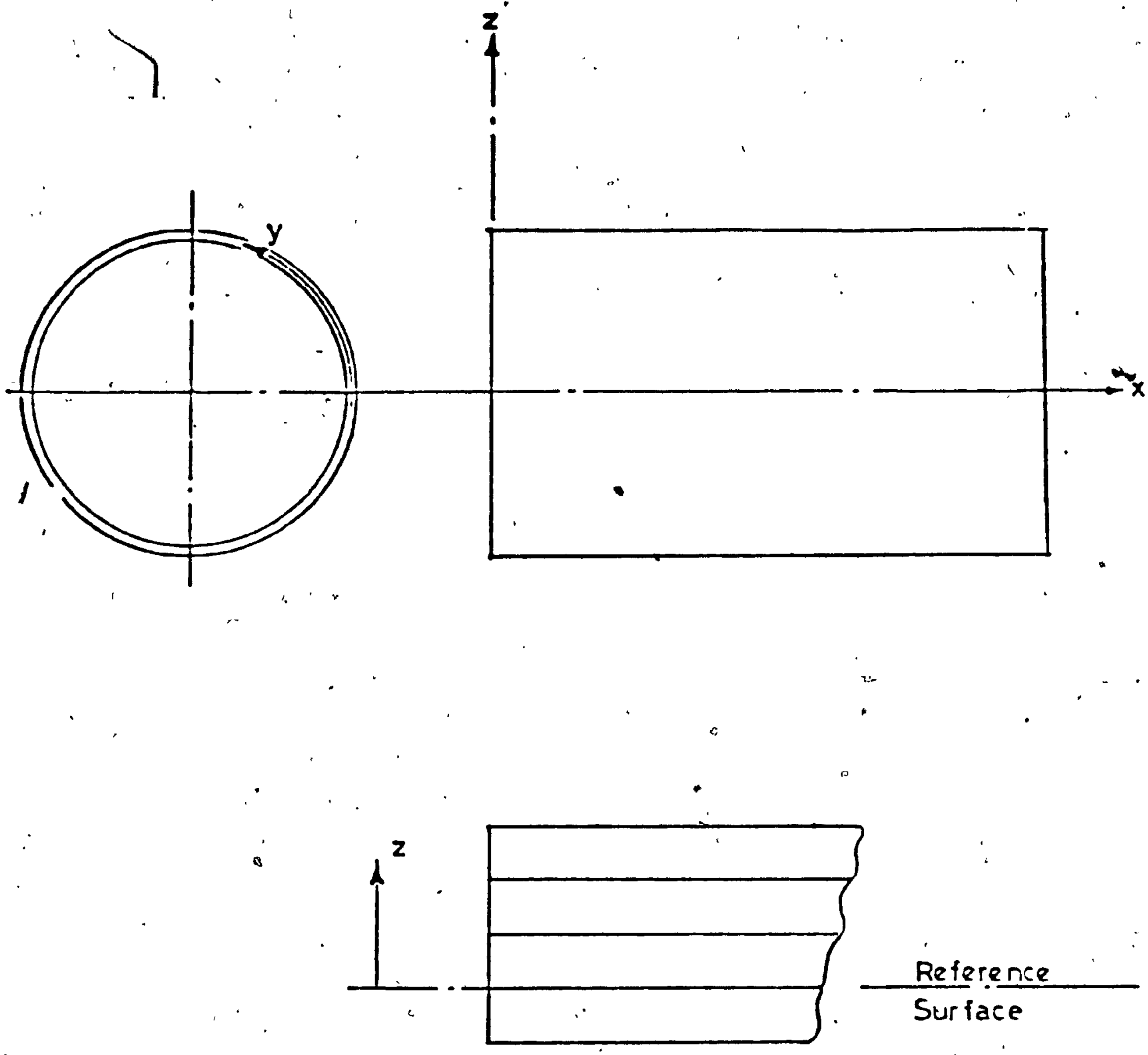

FIG 13 CURVILINEAR CO-ORDINATE SYSTEM [12]

(a) Uni Directional Composite

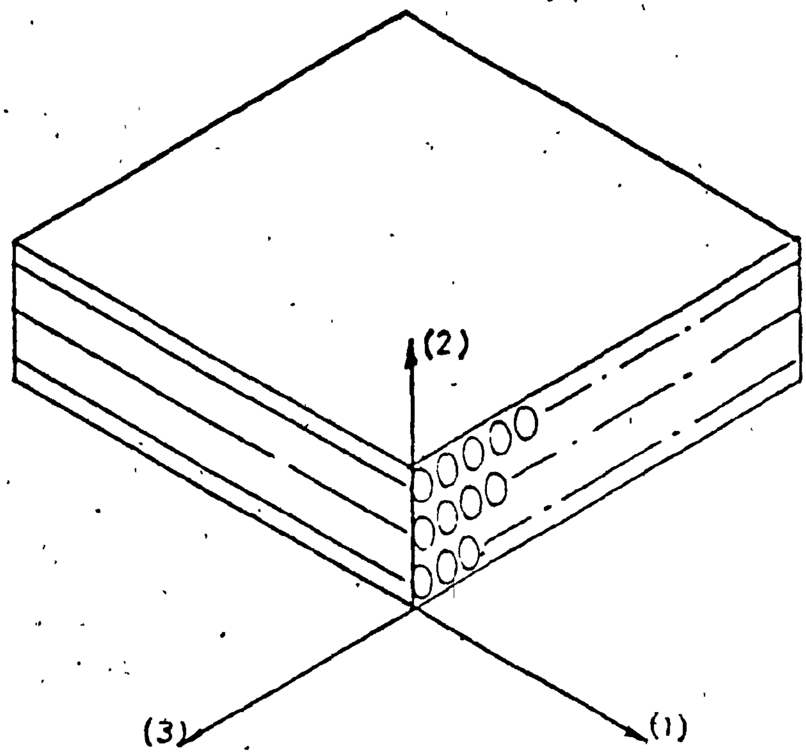

(b) Axis Rotation

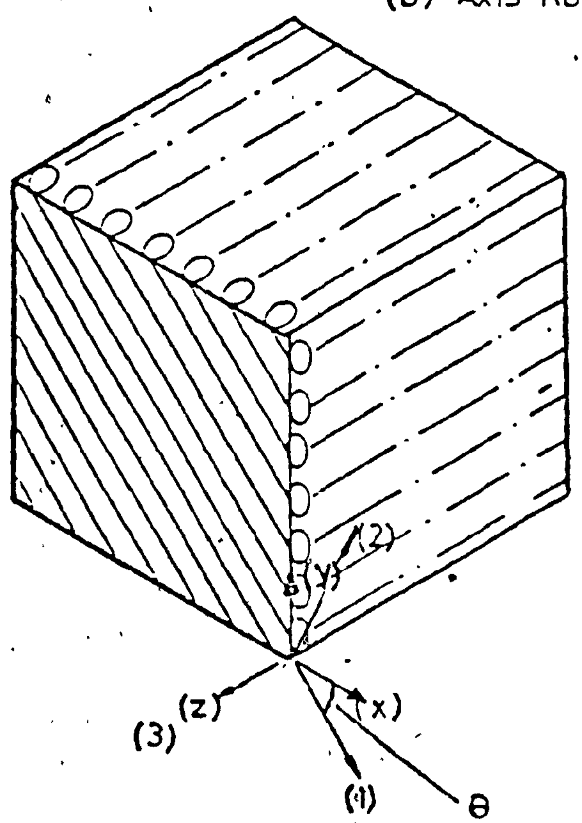

FIG 14· CO-ORDINATE SYSTEMS (FILAMENTARY) [12]

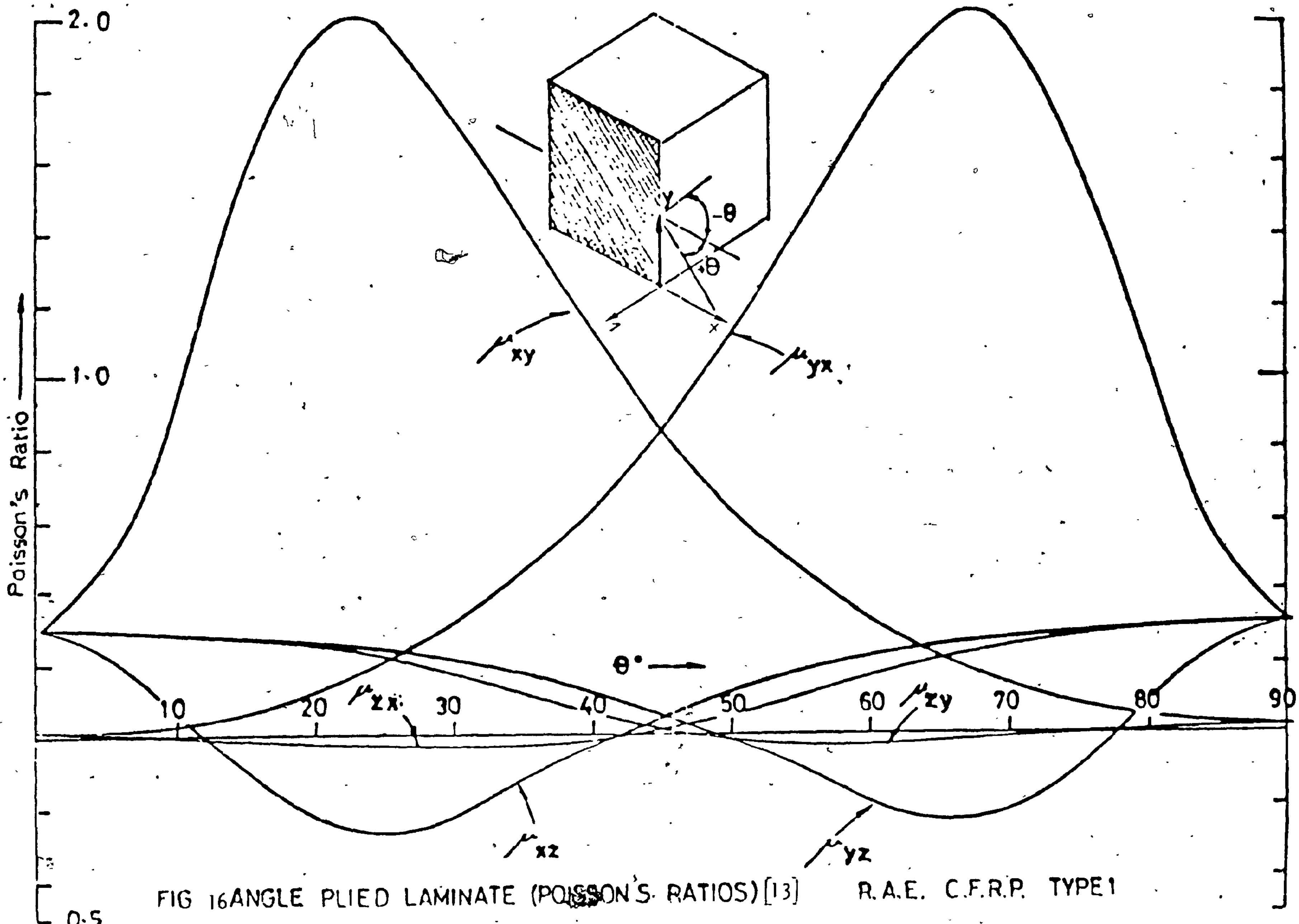

FIG 16 ANGLE PLIED LAMINATE (POISSON'S RATIOS) [13] R.A.E. C.F.R.P. TYPE 1

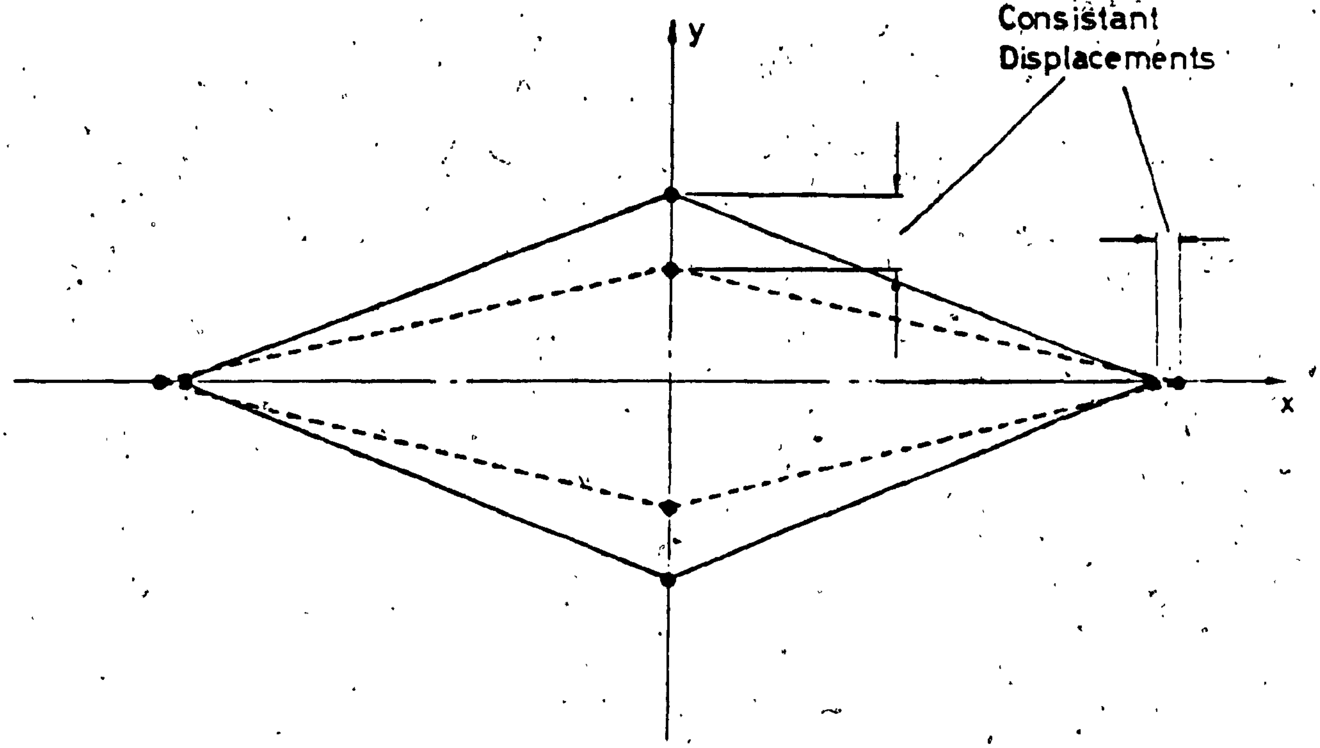

FIG 17 FOUR BAR CHAIN [13]

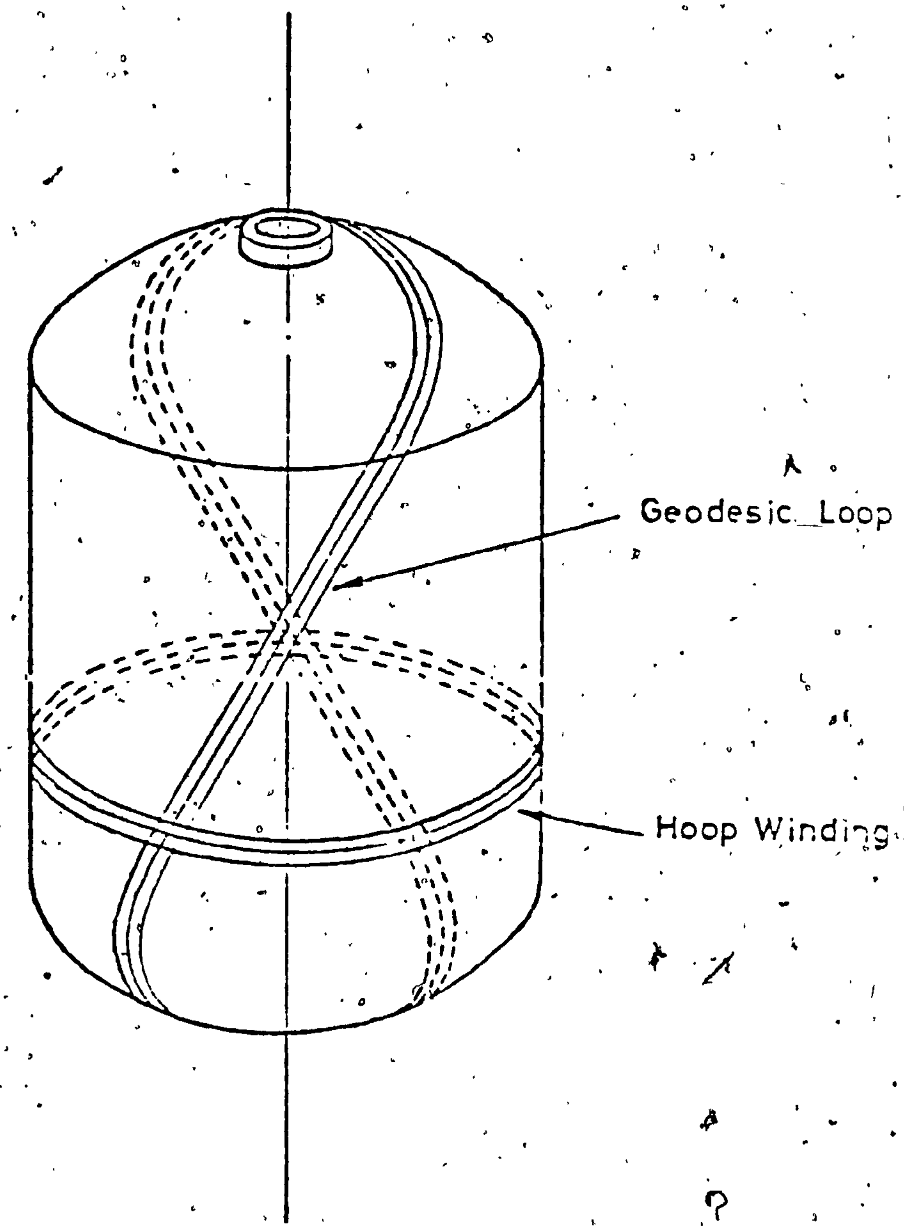

FIG 18 TYPICAL FILAMENT WOUND PRESSURE BOTTLE [13]

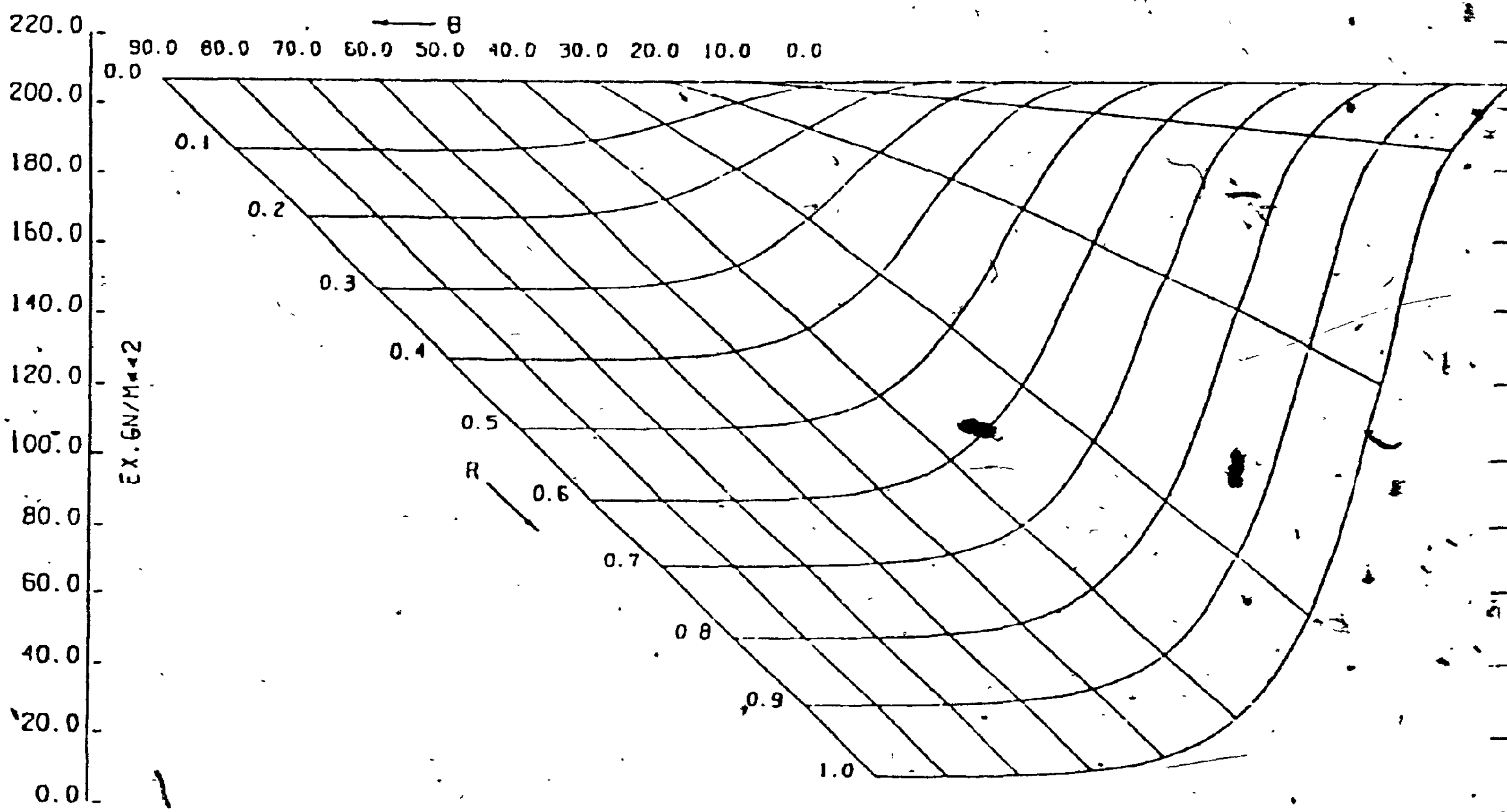

FIG 19 LONGITUDINAL ELASTIC MODULUS EX
(R.A.E. C.F.R.P. TYPE 1) [13]

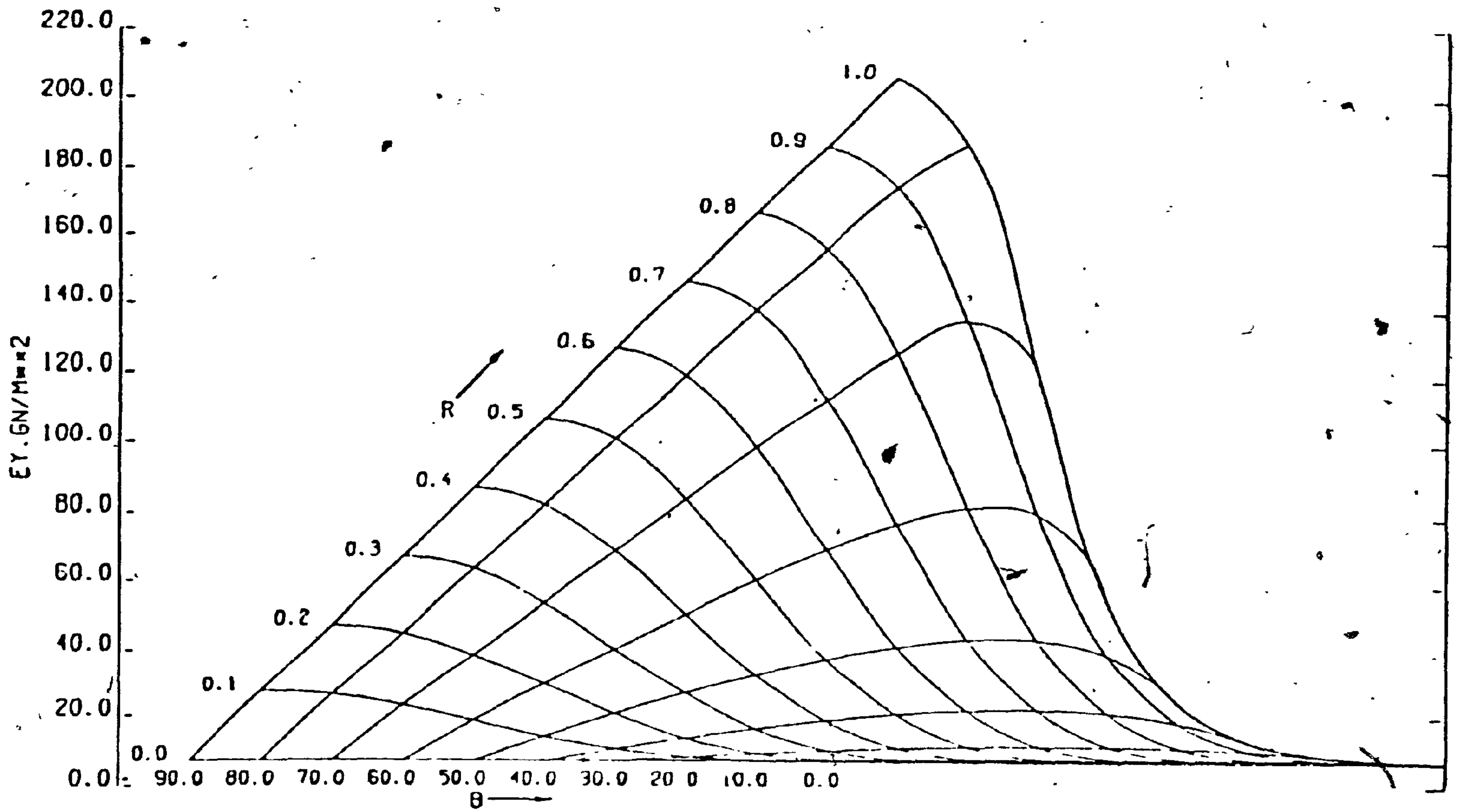

FIG 20 TRANSVERSE ELASTIC MODULUS EY
(R.A.E. C.F.R.P. TYPE 1) [13]

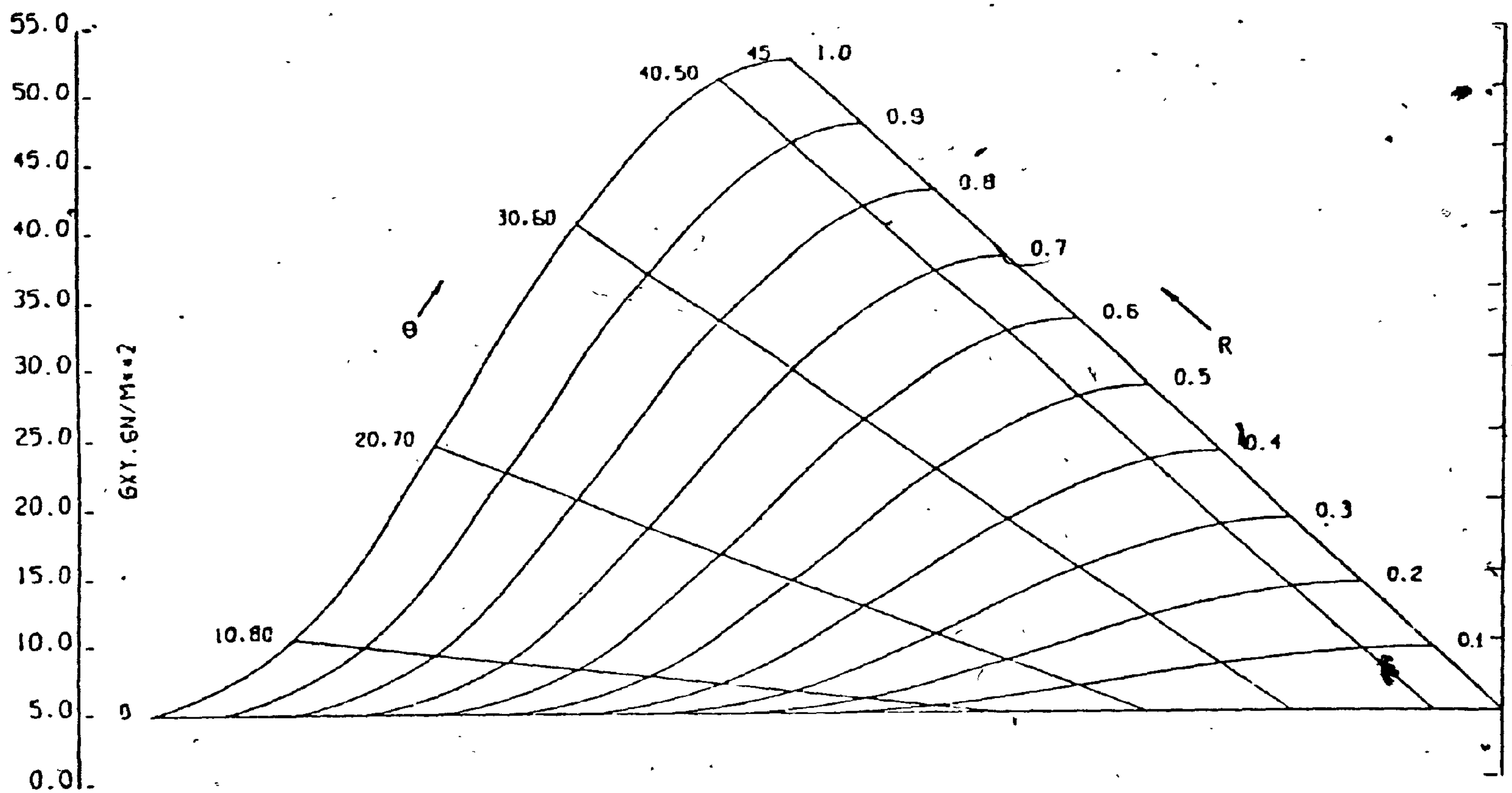

FIG 21 SHEAR MODULUS GXY
R.A.E. C.F.R.P. TYPE 1 [13]

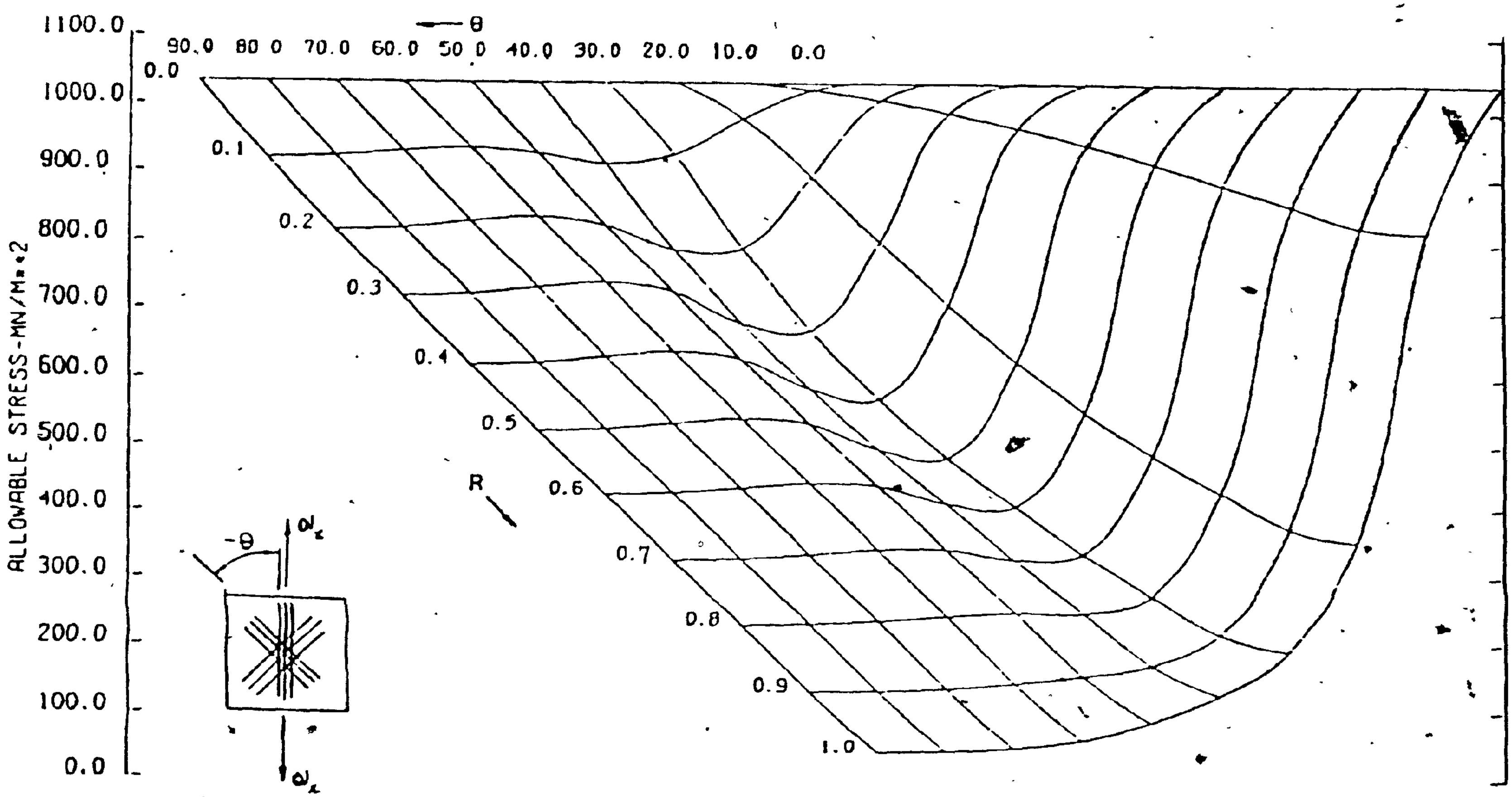

FIG 22 STRENGTH CHART (HOOPTENSION ONLY)
(R.A.E. C.F.R.P. TYPE 1) [13]

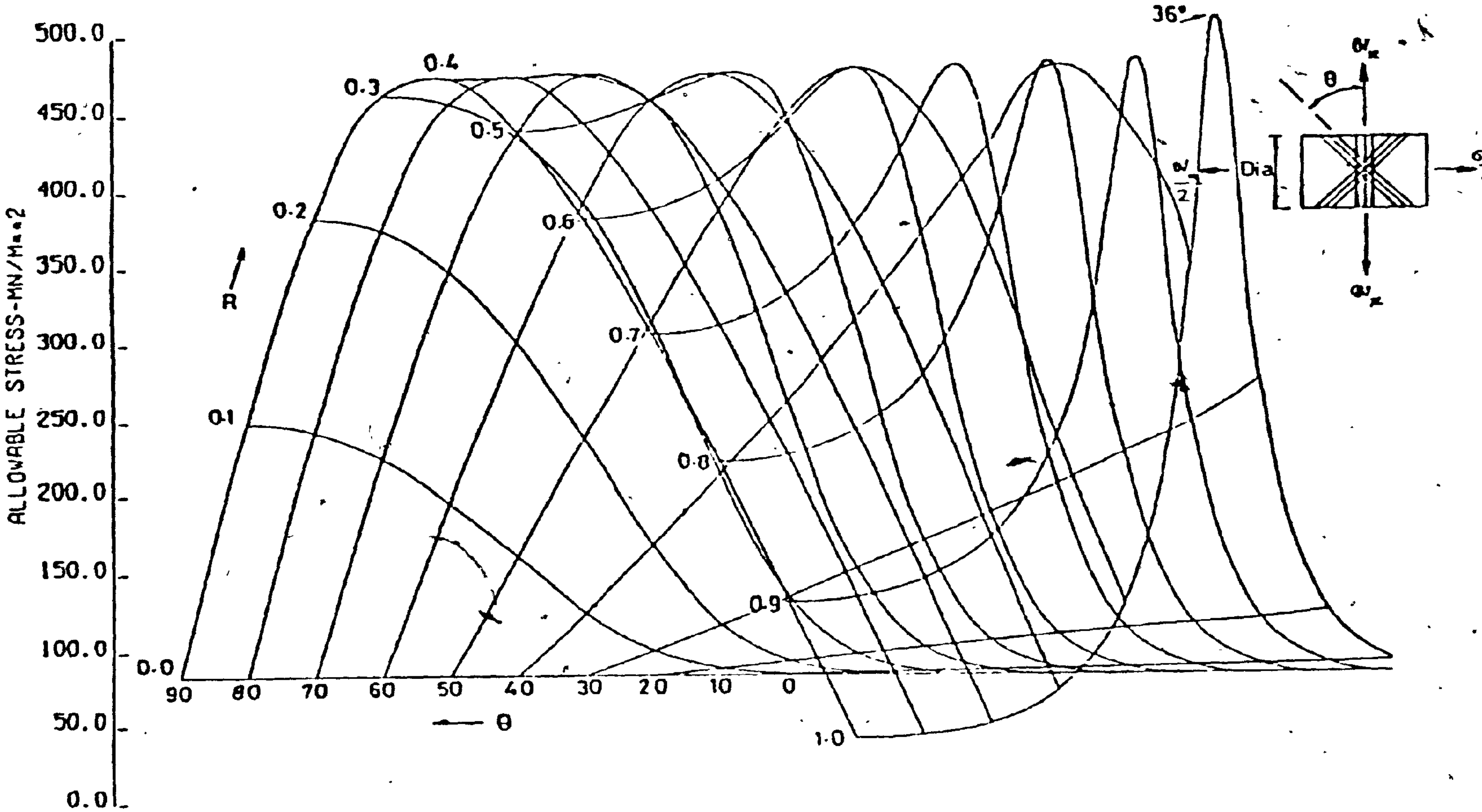

FIG 23 STRENGTH CHART (BIAXIAL STRESS RATIO =2)
(R.A.E. C.F.R.P. TYPE 11 [13]

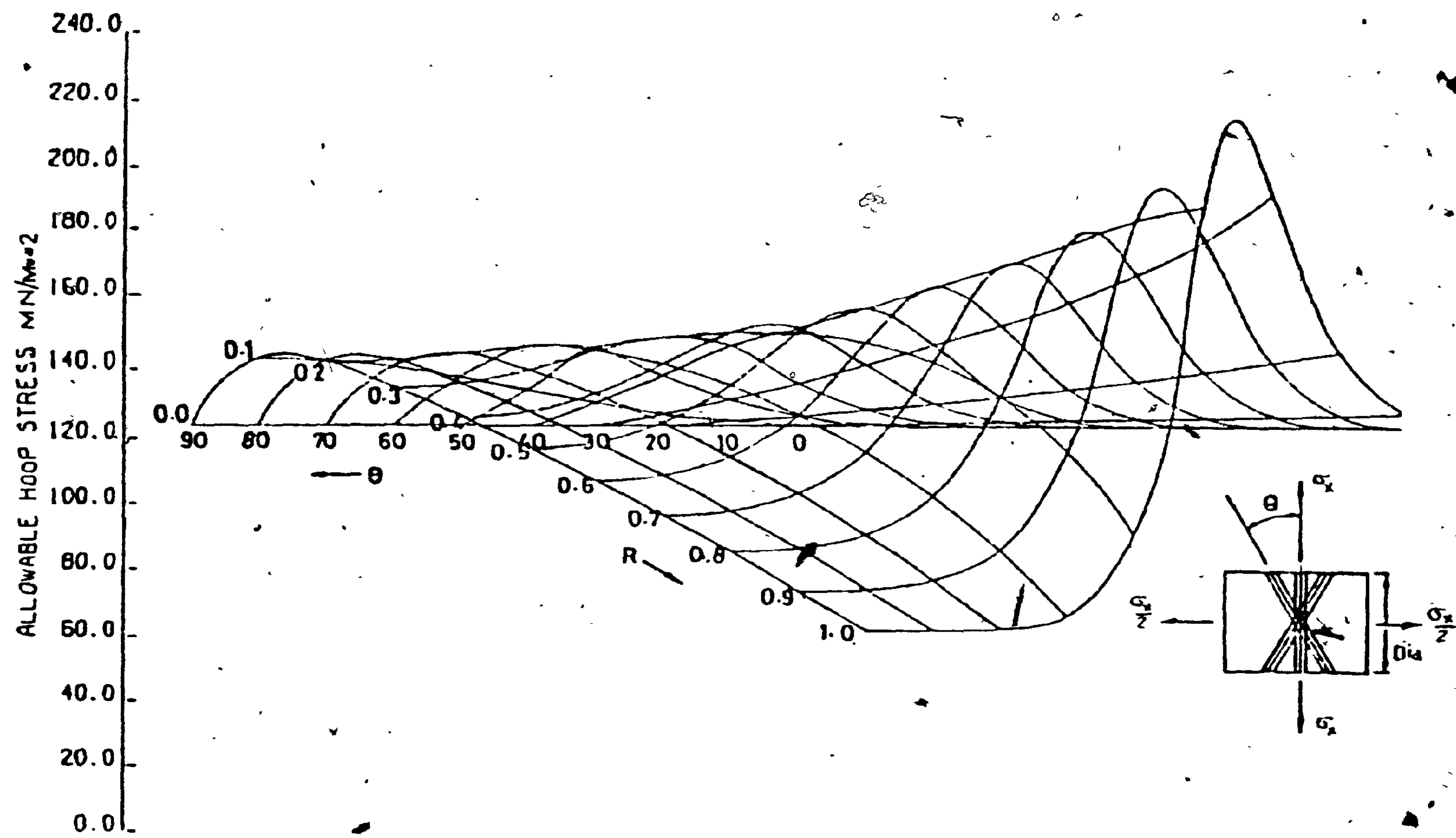

FIG. 24 STRENGTH CHART (BIAXIAL STRESS RATIO =2)
(3M G.F.R.P. 3M-XP215S)_Continuum Analysis [13]

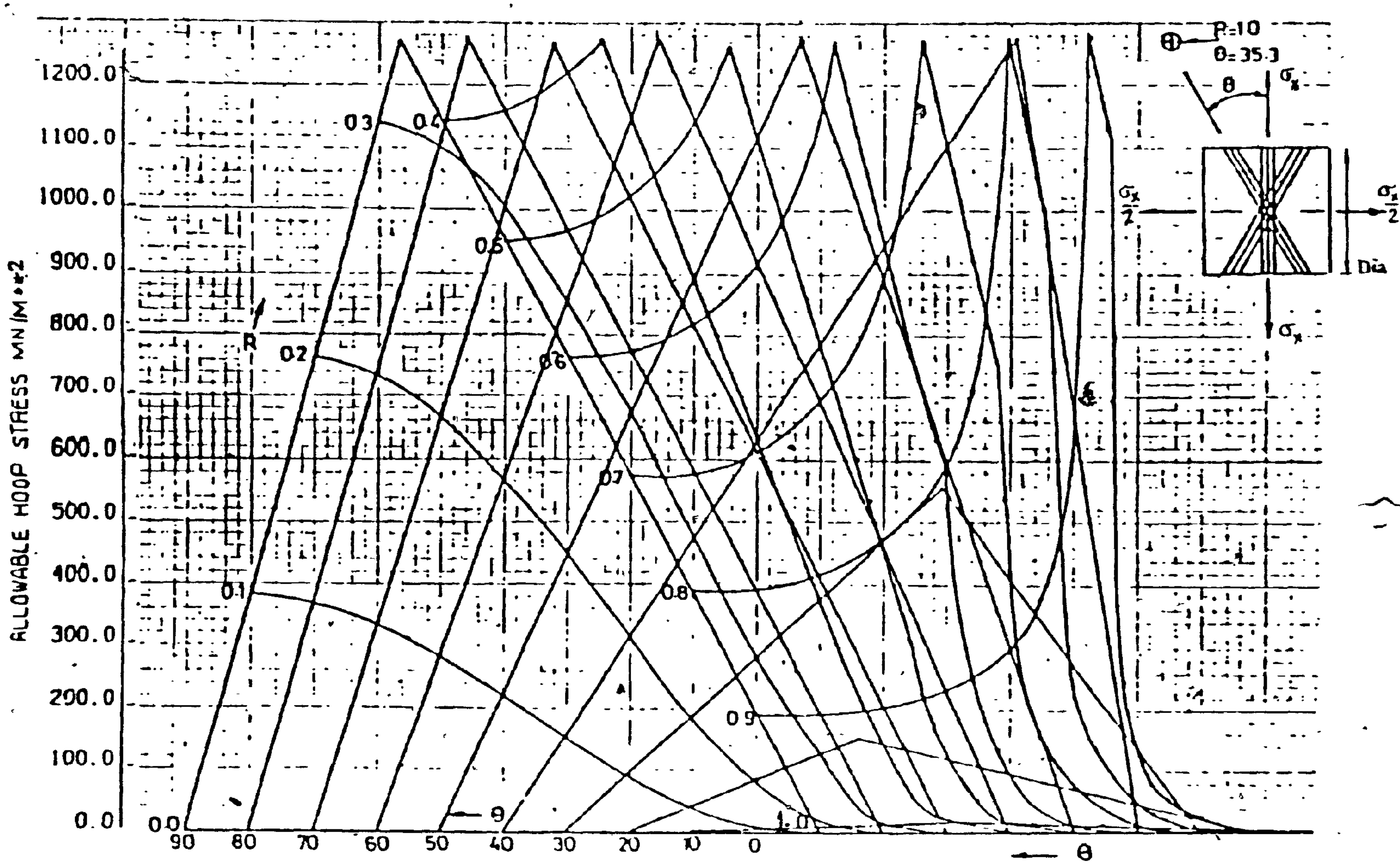

FIG. 25 STRENGTH CHART (BIAXIAL STRESS RATIO =2)
(3M G.F.R.P. 3M-XP215S NETTING ANALYSIS) [13]

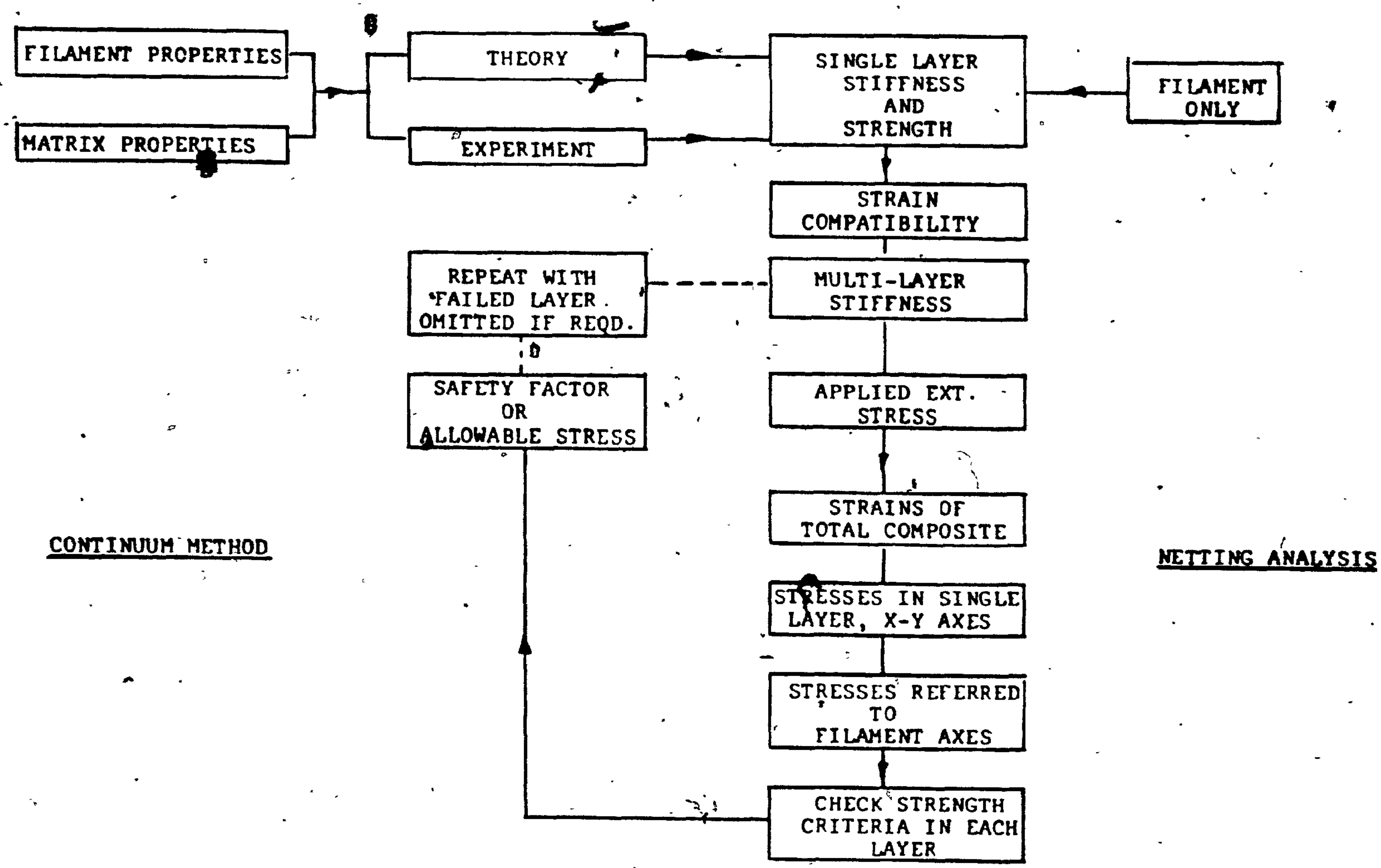

Fig. 26 Strength and stiffness flow chart [13]

MATERIAL	E_l	E_t	G_{lt}	μ_{lt}	σ_l tens	σ_l comp	σ_t tens	σ_t comp	τ_{lt}	ρ'	V.F.
	GN/m^2				MN/m^2					$Kg/m^3 \times 10^3$	%
R.A.E. C.F.R.P. Type 1	207.0	7.58	4.83	0.3*	1033	828	41.4*	41.4*	55.2	1.492	60
R.A.E. C.F.R.P. Type 2	127.3	7.58	5.52	0.3*	1310	828	41.4*	41.4*	69.0	1.492	60
THORNEL C.F.R.P. 75S	310.0	6.20	5.10	0.32	1478	670	31.8	186.0	41.4	1.492	60
HERCULES C.F.R.P. HTS	145.0	9.65	4.90	0.25	1408	1380	76.0	234.0	96.5	1.492	60
DU.PONT PRD-49	75.8	5.52	2.07	0.34	1276	276	29.6	138.0	44.1	1.385	60
- BORON R.P.	220.0	20.7	6.90	0.21	1297	2840	62.7	310.0	62.0	1.940	60
SCOTCHPLY G.F.R.P. Type 1002	39.3	9.65	2.69*	0.264*	1102	620	20.0	138.0	29.6	1.80	45
R.A.E. G.F.R.P.	46.3	7.17	2.69*	0.264	1138	635	27.6*	112.0*	53.8	1.910	54
3M G.F.R.P. 3M-XP215S	55.0	18.55	2.76*	0.27*	1904	690	62.1	202.0	68.2	1.950	-

* assumed values

TABLE 14 MATERIAL PROPERTIES (S.I. UNITS) UNIDIRECTIONAL FIBRE REINFORCED PLASTICS. [13]

CHAPTER (5)

CONCLUSION AND FUTURE WORK

Advanced filament wound pressure vessels are the result of applying aerospace materials and processes to manufacture useful commercial products. The transfer of technology has been successful by carefully retaining the essential parameters of the technology while modifying those that cause high costs characteristic of the aerospace industry. Thus, advanced technology but lower cost commercial composite pressure vessels are now available for military/aerospace applications. As it has been discussed earlier there are different matrices and reinforcing fibers commonly used in fiber reinforced plastic pressure vessels, different vessel compositions and fabrication techniques, also there are two different philosophy in analytical analysis in verifying the structural integrity of FRP pressure vessels.

However, there is still further work to be done to encourage more usage of fiber reinforced plastics pressure vessels in our daily life. Because of the lack of a complete design code, reliable design should be based on thorough stress analysis and costly tests, thus engineering costs for FRP equipment is higher than for analogous steel equipment.

A comprehensive design code should be formulated and adopted by users and fabricators. It should provide a step by step design procedure. This will reduce engineering costs, and reduce misunderstanding between fabricators and purchasers. Fabrication techniques are not standardized so that here is large variability in mechanical properties of the laminates in equipment. This variability must be accounted for in design.

Improvement of design methods would be accelerated, if creep data on common FRP laminates were available. Reliability will be improved by better non destructive proof test methods, such as acoustic emission.

Improvements in filament wound pressure vessels will result from the application of new materials and fabrication process innovations in the form of high modulus, high strength filaments, lighter weight metal liner, studies of advanced bonding systems, novel fabrication techniques such as adhesive bonding of liner segments, and new welding methods.

More studies needed to better define the safe fatigue life of vessels by studing the crack propagation characteristics as well as their behaviour under cycling loads also elasticity analysis of stress concentrations caused by openings, vibrations, buckling and thermal-elasticity should be investigated.

The added knowledge of the structural behaviour of FRP pressure vessels will provide a better basis of design and manufacturing processes.

Fiber reinforced plastics pressure vessels without doubt will offer the choice of a major step forward in terms of weight reduction and safe operation and one can foresee their increasing utilization in our daily life.

REFERENCES

1. E.E. Morris, W.P. Paterson, R.E. Landes and R. Gordon "Composite Pressure Vessels for Aerospace and Commercial Applications", Structural Composites Industries, Inc., Azusa, California, 1977

2. Edgar E. Morris "Commercial Filament Wound Pressure Vessels for Military and Aerospace Applications" SCI, Azusa, California, SAE 811093, 1981

3. E.E. Morris "Glass Fiber Reinforced Metallic Tanks for Cryogenic Service" NASA-CF-72224, Lewis Research Center, 1967

4. J.N. Fleck and K.R. Hanby "High Performance Fiber Reinforced Polymers" Metals and Ceramics Information Center, Columbus, Ohio, 1977

5. T.T. Chiao, M.A. Hamstad, E.S. Jessop and R.H. toland "High Performance Fiber/Epoxy Composite Pressure Vessels" NASA-CF-159512 1978

6. R.F. Lark "Recent Advances in Lightweight, Filament Wound Composite Pressure Vessel Technology" NASA-TM-73699, 1977

7. R. Tetlow "Design and Testing of Some Reinforced Plastic Components" Cranfield Institute of Technology, 1975

8. S. Timoshenko and S. Woinowsky Krieger "Theory of Plates and Shells" McGraw-Hill, New York, 1959

9. S.W. Tsai "Structural Behavior of Composite Materials" NASA-CF-71, 1964

10. S.W. Tasi and V.D. Azzi "Strength of Laminated Composite Materials" AIAA Journal, Vol, A, No. 2, 1966

11. R. Hill "The Mathematical Theory of Plasticity" Oxford University Press, London, 1950

12. R.C. Fews and R. Tetlow "Stress Analysis of Laminated Axisymmetric Cylinders" Cranfield Institute of Technology, Memo No. 7511, 1974

13. R.C. Fews and R. Tetlow "Design with Fiber Reinforced Materials" Cranfield Institute of Technology, Memo No. 7506, 1975

14. American Society of Mechanical Engineers (ASME) Boiler and Pressure Vessel Code Section 10

15. United States Department of Transport (DOT) Excemption DOT-E-8162

16. Military Standard for Fiber Reinforced Plastics Pressure Vessel MIL-T-25363